

**IOS**  
DEACON LABORATORY

DIRECTIONAL WAVE DATA RECORDED  
IN THE SOUTHERN NORTH SEA

BY  
C.H. CLAYSON & J.A. EWING

REPORT NO. 258  
1988

 Natural  
Environment  
Research  
Council

**INSTITUTE OF  
OCEANOGRAPHIC SCIENCES  
DEACON LABORATORY**

**INSTITUTE OF OCEANOGRAPHIC SCIENCES  
DEACON LABORATORY**

---

**Wormley, Godalming,  
Surrey, GU8 5UB, U.K.**

Telephone: 0428 79 4141  
Telex: 858833 OCEANS G  
Telefax: 0428 79 3066

*Natural Environment Research Council*

INSTITUTE OF OCEANOGRAPHIC SCIENCES

DEACON LABORATORY

REPORT No. 258

Directional wave data recorded  
in the southern North Sea

C.H. Clayson & J.A. Ewing

1988

*The preparation of this report was supported financially by the Department of Energy.*



DOCUMENT DATA SHEET

<p><i>AUTHOR</i>      CLAYSON, C.H. &amp; EWING, J.A.</p>	<p><i>PUBLICATION DATE</i>    1988</p>
<p><i>TITLE</i>                      Directional wave data recorded in the southern North Sea.</p>	
<p><i>REFERENCE</i>              Institute of Oceanographic Sciences Deacon Laboratory, Report, No.258, 70pp.</p>	
<p><i>ABSTRACT</i></p> <p>A directional wave buoy was deployed 11 nm north-east of Cromer, in the southern North Sea during the period from December 1985 to June 1987. The deployments of the Datawell WAVEC buoy were carried out on behalf of the U.K. Department of Energy.</p> <p>This report summarizes the techniques used and results obtained during the measurement period. The basic non-directional information consists of measurements of the frequency spectrum from which wave height and period statistics have been computed. In addition to this information, the directional wave buoy provides estimates of the directional spectrum from which the mean wave direction and directional spread are calculated.</p> <p>The results of this study are contained in a set of tables and figures which, in addition to wave height and period statistics, provide statistics of the joint occurrence of wave height, wave period and wave direction. Information is given for each of four seasons and for the whole data set.</p>	
<p><i>ISSUING ORGANISATION</i></p> <p style="text-align: center;">Institute of Oceanographic Sciences Deacon Laboratory Wormley, Godalming Surrey GU8 5UB. UK.</p>	<p><i>TELEPHONE</i>      0428 79 4141</p> <p><i>TELEX</i>            858833 OCEANS G</p> <p><i>TELEFAX</i>        0428 79 3066</p>
<p><i>KEYWORDS</i></p> <p style="text-align: center;">DATA BUOY (WAVE)      DIRECTIONAL WAVE SPECTRA WAVE DATA          WAVE DIRECTION      NORTH SEA</p>	<p><i>CONTRACT DEN</i> No.E/5B/CON/935/2043</p> <p><i>PROJECT</i></p> <p><i>PRICE</i></p> <p style="text-align: right;">£19.00</p>



<u>CONTENTS</u>	Page
INTRODUCTION	7
LOCATION	8
INSTRUMENTATION AND DATA COLLECTION	10
Buoy configuration	10
Buoy sensors	10
Sampling and telemetry	12
Reception and real time processing	13
Data translation and transfer to IBM	18
Calibrations	19
Accuracy of measurements	21
ANALYSIS AND RESULTS	24
Definition of parameters	24
Sampling variability	25
Data return	25
Distribution and return value of significant wave height	25
Joint distribution of wave height and period	26
Joint distribution of wave height and direction	26
Joint distribution of wave period and direction	26
Joint distribution of wave height, period and direction	27
Distribution of directional spread parameter	28
ACKNOWLEDGEMENTS	28
REFERENCES	29
APPENDIX A.1: Deployment history of Cromer Wavecs	30
APPENDIX A.2: Method of analysis and definition of directional parameters	33
APPENDIX A.3: Summarised calibrations of Wavecs	35
APPENDIX A.4: Influence of currents on the check ratio	37
TABLES 3-9	38
FIGURES 3-7	56





## 1. INTRODUCTION

This report summarises the techniques used and the results obtained during a 19 month series of deployments of a Datawell Wavec directional wave buoy, 11 nm north-east of Cromer, Norfolk during the period from December 1985 to June 1987. The deployments were carried out as part of a programme of work, commissioned by the U.K. Department of Energy Petroleum Engineering Department, for Directional Wave Measurements in the Southern North Sea. This report is the first directional wave data report of its type, involving the Wavec equipment, to be produced by the Institute of Oceanographic Sciences Deacon Laboratory. Therefore, considerably more detail on the techniques has been included, for reference in the event of the production of further directional wave data reports.

The location of the buoy mooring, described in 2 below, was selected with a view to investigating the propagation of waves from the North, over a series of banks between the Dogger Bank and the Southern gas fields Hewitt and Leman. These banks are predominantly orientated North West - South East. The buoy mooring was close to the Hewitt field.

The activities reported upon include:-

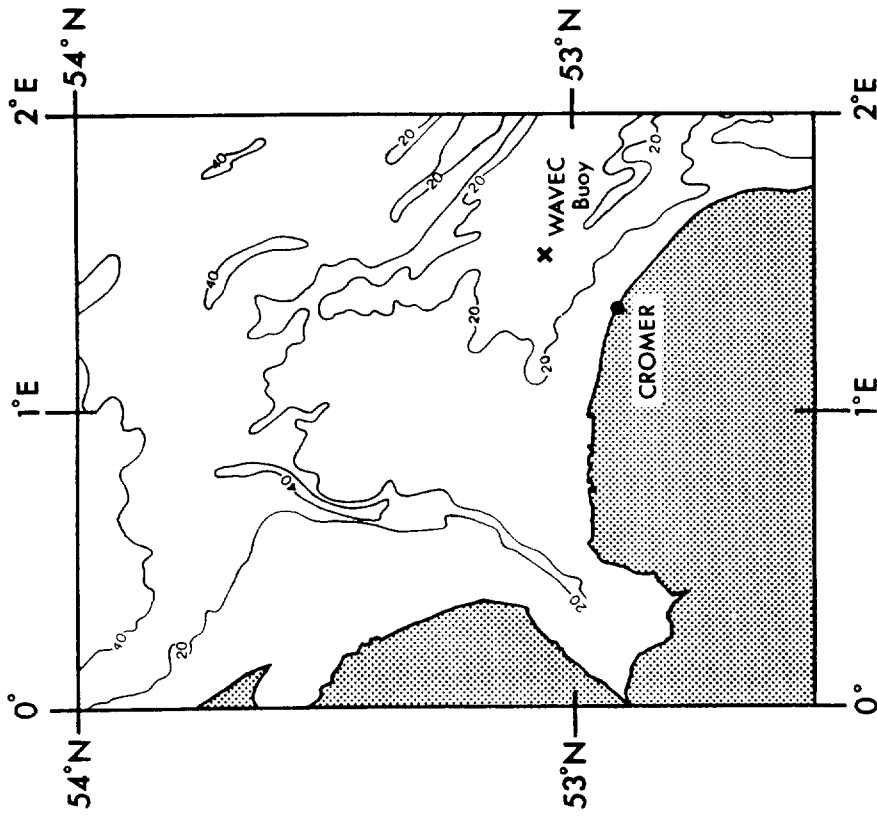
- (a) the deployment, recovery, maintenance and calibration of the buoys used. This was subcontracted to Hydraulics Research Ltd;
- (b) the establishment, operation and maintenance of the shore based receiving station and real time processing equipment and logging equipment. This was carried out by IOSDL with the considerable assistance of the local HM Coastguard Sector Officer;
- (c) the translation, quality checking and reformatting of the field processed data tapes and the transfer of the data to the IBM mainframe computer at Wallingford (carried out by IOSDL);
- (d) the conversion of the data transferred to the IBM to the standard MIAS directional wave data format (carried out by MIAS at the Proudman Oceanographic Laboratory);
- (e) the production of summarised data in graphical and tabular parameterised form from the complete MIAS data set (carried out by IOSDL).

## 2. LOCATION

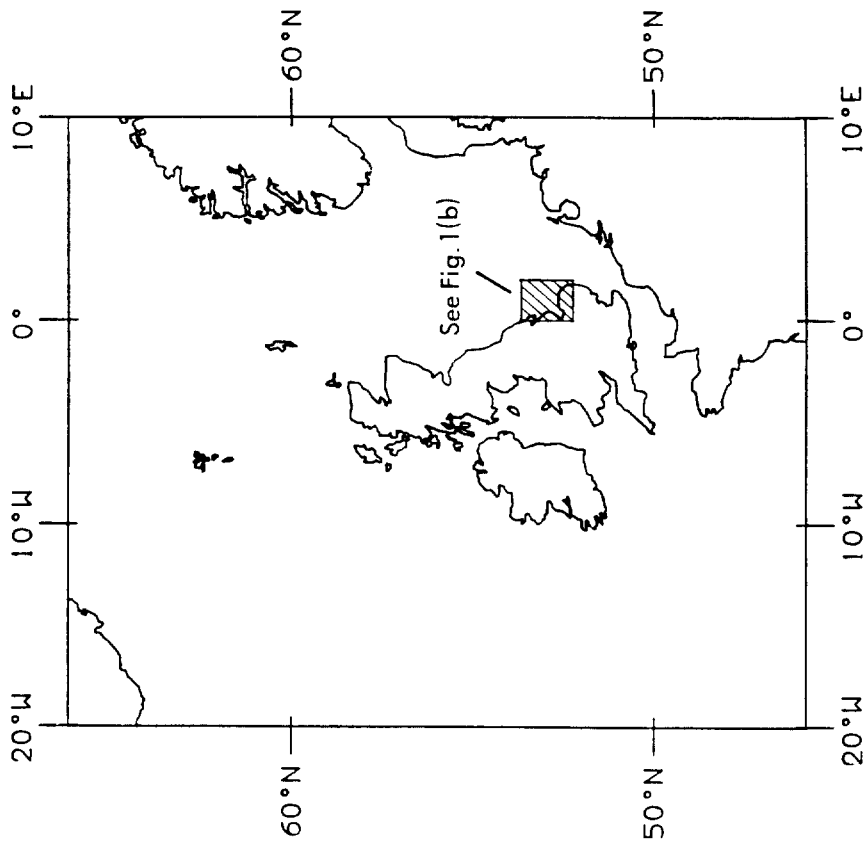
The wave measurements were made with a Datawell Wavec buoy moored at 53°04'N, 1°31'E, 11 nm north-east of Cromer, as shown in Figs. 1(a) and (b). The water depth at the location of the buoy was 31 m.

The bathymetry in the vicinity of the buoy is shown in Fig. 1(b); there are a series of banks, with depths less than 20 m, lying to the north-east of the location, which extend to a distance of about 30 nm. A large area of shallow water off the Wash lies to the north-west where the depth is less than 20 m.

The mean spring tidal range at the site is 5 m. Tidal currents in the area are predominantly semi-diurnal and are aligned approximately south-east to north-west with a maximum speed of about 0.9 m/sec.



(a)



(b)

Fig. 1: Location of WAVEC directional wave buoy off Cromer. Depths in metres.

### 3. INSTRUMENTATION AND DATA COLLECTION

Two buoys were dedicated to this project, so that a spare was always ready for use. These were standard Wavec buoys with serial numbers 22011 (owned by the Department of Energy, procured by IOS from Datawell by in March 1985) and 22025, procured by HR Ltd in October 1985. The two buoys were in the care of HR Ltd for the duration of the contract for their deployment (NERC F3/B1/67) from November 1985 to August 1987.

#### 3.1 Buoy configuration

The Wavec buoy consists of a discus-shaped float of synthetic foam, with central stainless steel instrumentation canister, top float (for self righting) fitted with navigational light, transmitting antenna and mooring system (figure 2). The discus float is assembled from four 90° segments, for ease of transport. These segments are clamped between four radial wings, pinned to the central instrumentation housing, by a tensioning system of synthetic cords, webbing and rubber strainers; this system is also used to secure the top float. The resulting assembly is 2.5 m in diameter and 1.7 m in height, not including the transmitting antenna, and weighs 650 kg in air (710 kg including mooring cross).

The flotation unit is designed to follow the water surface, accurately, in both displacement and in slope, up to a frequency of about 0.5 Hz. The buoy natural heave frequency is 0.61 Hz and its natural pitch-roll frequency is 0.72 Hz. The responses are well damped. The shape of the hull not only contributes to the damping (since the chine dissipates energy by wave radiation) but also minimises static tilts of the buoy hull due to current, since the moments of drag forces about the effective mooring point at the centre of buoyancy are well balanced. Although the centre of buoyancy is actually situated within the instrumentation canister, mooring tension is transmitted to the buoy via the mooring cross which effectively translates the tension to pass through the centre of buoyancy, thereby avoiding any moments which would cause slope-following errors.

#### 3.2 Buoy sensors

The buoy sensors are all contained within the instrumentation canister and include a "Hippy 120" heave, pitch and roll sensor and a 3-component

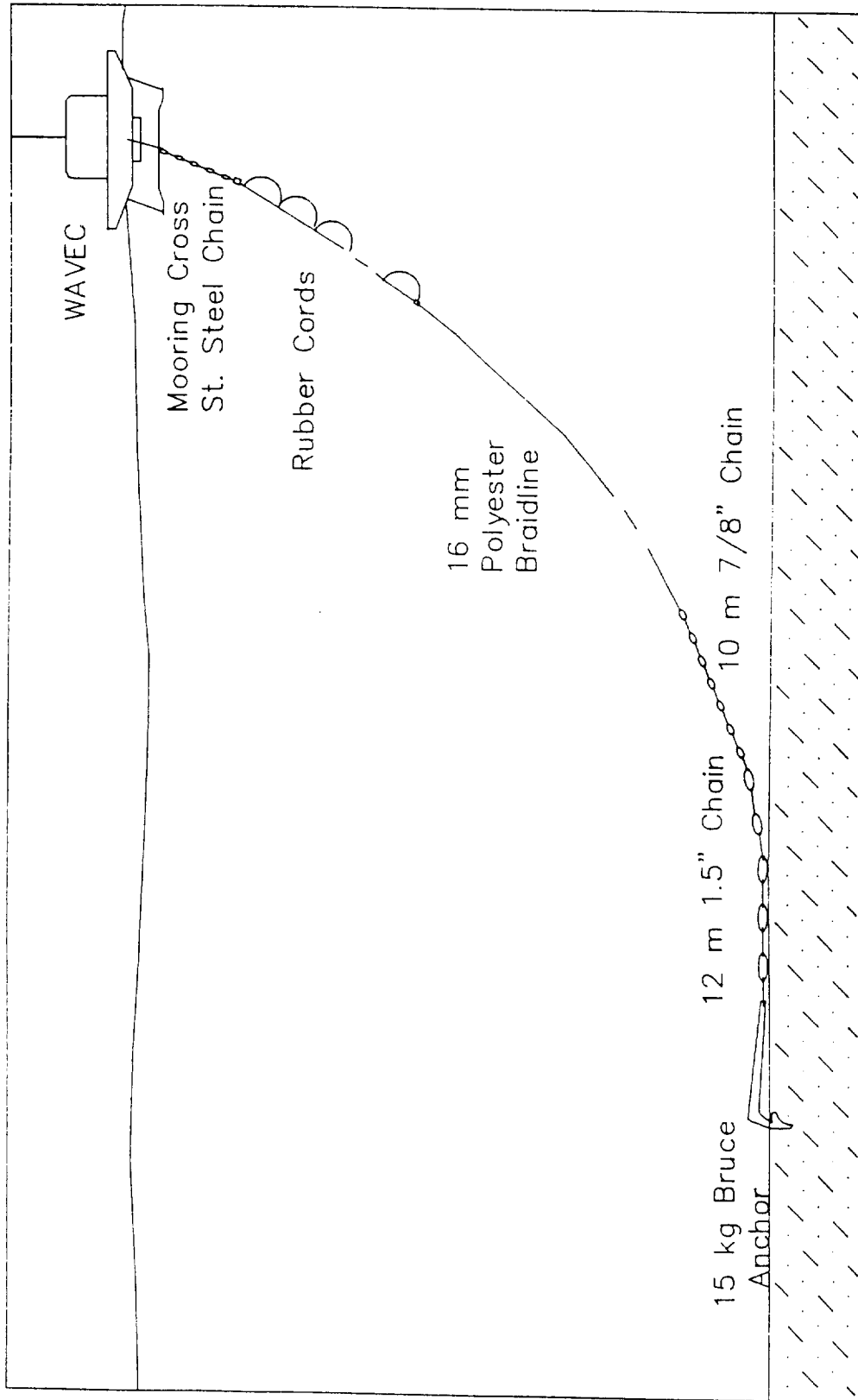


Fig. 2: Schematic of Cromer WAVEC mooring (not to scale).

strapped-down fluxgate magnetometer. The "Hippy 120" uses an improved form of the fluid suspension system used in the Waverider buoy to achieve a stabilised platform with 120 second natural period. In addition to the vertical accelerometer sensor, the platform carries a coil which senses components of two orthogonal alternating magnetic fields whose directions are fixed relative to the buoy hull, thereby providing signals proportional to the sine of the buoy pitch and to the sine of the buoy roll angle, respectively. These angles, in combination with the three magnetometer signals proportional to the Earth's magnetic field components in the buoy "vertical" axis, pitch axis and roll axis, are used to derive the buoy float slopes in the North-South and East-West planes, including the vertical.

### 3.3 Sampling and telemetry

The Hippy acceleration signal is doubly integrated to a displacement signal, using integrators including a high pass filter to cut out low frequency error signals. The transfer response of this filter is given by

$$H_1(s) = \frac{s^2}{s^2 + \sqrt{2}\omega_0 s + \omega_0^2} \cdot \frac{s}{s + \omega_0}$$

$$\text{where } \omega_0 = 2\pi/30.8, \omega_0 = 2\pi/170.$$

This is, therefore, a combination of a maximally-flat (Butterworth) 2nd order high pass filter, with a cut-off at 30.8 second period, and of a single pole high pass filter with a cut-off at 170 seconds period.

The heave, pitch, roll, Hx, Hy and Hz magnetometer signals are then anti-alias filtered by six identical 7th order low pass filters, having amplitude transfer response

$$|H_2(\omega)| = (1 + (0.265\omega)^{14})^{-\frac{1}{2}}$$

Note that the phase response of the anti-alias filters is unimportant, since all channels are similarly affected.

The six filtered channels, together with buoy battery voltage (which is steady and needs no anti-alias filtering) are then simultaneously sampled at 1.28 Hz, using sample and hold circuits, and sequentially digitised to 12 bit offset binary form (2048 = zero voltage, 4048 = +full scale voltage, 48 = -full scale voltage).

The data scales are as follows:

		<u>digits</u>
Heave	+2000 cm	4048
	0 cm	2048
	-2000 cm	48
Pitch or Roll	$\sin (+\pi/2)$	4048
	$\sin (0)$	2048
	$\sin (-\pi/2)$	48
Hx, Hy and Hz	50 A/m	4048
	0 A/m	2048
Battery Voltage	26V (new)	1094
	14V (nearly exhausted)	1534

The seven channels are transmitted in the binary format, together with a sync channel (4095) and 11 bit and 10 bit check words as a 106.21 BCH code, having an error correction capability of 3 bits. Frequency shift keying of the r.f. carrier is used. The allocated frequency was 29.825 MHz.

### 3.4 Reception and real time processing

The digital transmissions from the buoy were received by a quarter-wave whip antenna with ground plane elements erected in the HM Coastguard Lookout compound at Cromer. The standard DIREC receiver/processor was used to decode and process the data, under the control of an HP85B microcomputer. The latter was used to read out and reformat the spectral processed data, together with housekeeping data, and to output the data to a Data Technology Tracker 1600 magnetic tape cartridge drive, at intervals of  $1\frac{1}{2}$  hours. The tapes were then

posted to IOS for translation, checking and transfer to the IBM mainframe at Wallingford.

The DIREC unit at Cromer first decodes the data and check bits. If 3, or less, bit errors occur in a transmitted frame (127 bits), these are corrected. If 4 errors occur, correction is not possible and the data is not modified. However, if 5 or more errors occur, there are three possibilities; in 83% of cases the errors are flagged but the data is not modified. In 17% of cases an invalid correction is made but, in 1 in  $10^6$  cases with 7 or more errors, no error will be detected. Clearly the last case is unlikely to happen without a considerable proportion of data also being detected as in error. Additional quality checks on the data are carried out on every sample. These include:

- (a) azimuth changes by less than  $15^\circ$ /second;
- (b) resultant magnetic field  $H_{abs} (= \sqrt{H_x^2 + H_y^2 + H_z^2})$  changes by less than 10% from its mean value averaged over each 256 "good" samples;
- (c) magnetic inclination (angle of dip) changes by less than  $5\frac{1}{2}^\circ$  from its mean value averaged over each 256 "good" samples;
- (d) heave changes by less than some excessive amount between samples.

Data on these checks and on transmission errors are included with the real time MONITOR data (raw data) and REAL data (transformed slope data) outputs, which can be monitored via an RS232 port. In the case of spectral data, the HP85B repeatedly examines the DIREC real time clock until it reaches one of the times for spectral analysis to begin, e.g. 0000 hours, 0130 hours, 0300 hours, ----, 2230 hours. The HP85B then commands the DIREC to commence spectral processing. This is done over a period of 30 minutes, using 9 ensembles of 256 samples of each time series (heave -1, slope NS -2, slope EW -3). Only data which passes the quality checks is used. The first and last 32 samples in each ensemble are tapered, using a cosine taper, to reduce leakage effects. The data are then transformed to the frequency domain using FFT and the nine



possible co- and quad-spectra are computed,

$$\begin{aligned}
 \text{i.e. } C_{11}(m) &= a_1^2(m) + b_1^2(m) & C_{22}(m) &= a_2^2(m) + b_2^2(m) \\
 & & C_{33}(m) &= a_3^2(m) + b_3^2(m) \\
 C_{12}(m) &= a_1(m)a_2(m) + b_1(m)b_2(m) & C_{13}(m) &= a_1(m)a_3(m) + b_1(m)b_3(m) \\
 & & C_{23}(m) &= a_2(m)a_3(m) + b_2(m)b_3(m) \\
 Q_{12}(m) &= a_2(m)b_1(m) - b_2(m)a_1(m) & Q_{13}(m) &= a_3(m)b_1(m) - b_3(m)a_1(m) \\
 & & Q_{23} &= a_3(m)b_2(m) - b_3(m)a_2(m)
 \end{aligned}$$

where  $a_n(m) + jb_n(m)$  is the  $m^{\text{th}}$  spectral estimate for time series  $n$ . Note that the frequency interval is  $1/(200 \text{ seconds})$ , i.e.  $0.005 \text{ Hz}$ .

These spectra are then averaged over all good ensembles and the results are normalised, corrected for tapering, heave integrator response (complex) and anti-alias filter response (modulus).

The following parameters are computed:

$$H_{\text{rms1}} = \sqrt{0.005 \sum_{m=10}^{127} C_{11}(m)} \quad \text{in cm}$$

the r.m.s. wave height from heave spectral estimates between  $0.05$  and  $0.635 \text{ Hz}$

$$H_{\text{rms2}} = \sqrt{\frac{\sum(H)^2}{N} - (\bar{H})^2} \quad \text{in cm}$$

the r.m.s. wave height from the heave time series of length  $N = 1800$  samples (nominal)

$C_{11 \text{ max}}$ , the maximum heave spectral estimate in  $\text{cm}^2/\text{Hz}$

$$\text{Heave offset} = \sqrt{C_{11}(0)/256} \quad \text{in cm}$$

$$\text{Slope offset} = \sqrt{(C_{22}(0) + C_{33}(0))/256} \quad (\text{tangent of angle})$$

The spectral data is output to the HP85B at the completion of processing in the form of a CQDATA message. This consists of 130 lines. The first line

is the time message,

e.g. \*1987 <sp> 3-21 <sp> 03:30 <sp> [xx xx xx]<CR-LF>  
year month-day time of end [unused hardwired  
of record timing parameters]

The second line is the LOG message

e.g. 0009,0000,0000,0000,0000,0000,0000,0000,0000,0000,0063<CR-LF>

This consists of eleven words with the following meanings

- word 1 Number of accepted ensembles.
- word 2 Number of missing samples within accepted series due to transmission errors or quality check failures (max. 10%).  
N.B. In the case of missing samples, slope values are replaced by zero, heave values are interpolated or replaced by zero.
- word 3 Number of gaps of  $\geq 2$  consecutive samples over the whole 30 minutes.
- word 4 Number of transmission error corrections over the whole 30 minutes.
- word 5 Number of uncorrectable samples over the whole 30 minutes.
- word 6 Number of samples where  $H_{abs}$  varied from mean by  $\geq 10\%$ , from  $|(H_{abs} - H_{abs})/H_{abs}|$  where  $H_{abs}$  is updated and averaged over each 256 "good" samples.
- word 7 Number of samples where azimuth changed by  $\geq 15^\circ$ /second.
- word 8 Number of samples where angle of dip varied from mean by  $\geq 5\frac{1}{2}^\circ$ , from  $|\text{inclination} - \text{inclination}|$  where inclination is updated and averaged over each 256 "good" samples.
- word 9 Number of samples where heave values passed only simplified quality check.
- word 10 Number of samples where heave was replaced by an interpolated value.
- word 11 r.m.s. waveheight in cm (calculated from time series, as above).

The next 128 lines are spectral data for spectral estimates 000 to 127 inclusive, but for the zero frequency estimates,  $C_{12}$ ,  $Q_{12}$ ,  $C_{13}$  and  $Q_{13}$  are meaningless and  $C_{23}$  is replaced by the spectrally-derived estimate of r.m.s. height  $H_{rms1}$  and  $Q_{23}$  is replaced by  $C_{11max}$ . The format of each line of spectral data is

LLL, $C_{11}$ , $C_{22}$ , $C_{33}$ , $C_{12}$ , $Q_{12}$ , $C_{13}$ , $Q_{13}$ , $C_{23}$ , $Q_{23}$ <CR-LF>

where LLL is the estimate number (000 to 127) and the estimates are in the format ±XXXXXE±XX.

The estimates are in the following units:-

$$\begin{aligned} C_{11}: & \text{cm}^2/\text{Hz} \\ C_{22}, C_{33}, C_{23}, Q_{23}: & 0.25 \times 10^{-6} \text{ rad}^2/\text{Hz} \\ C_{12}, C_{13}, Q_{12}, Q_{13}: & 0.5 \times 10^{-3} \text{ cm.rad}/\text{Hz} \end{aligned}$$

The original IOS HP85B control programme used at Flamborough Head requested spectral data at 3 hourly intervals and recorded all the above CQDATA, plus a single MONITOR message line, mainly as a check on battery voltage. It was found that this repeat interval was too long and it was changed to  $1\frac{1}{2}$  hourly. In order to keep the data rate more or less constant, the change to  $1\frac{1}{2}$  hourly data was accompanied by averaging over pairs of estimates in the HP85, so that only estimates 000, 001+002, 003+004 ..., 125+126 were logged on the tape drive. The frequency interval is, thus, 0.01 Hz for all of the Cromer data, with estimates at (0), 0.0075, 0.0175, 0.0275 ..., 0.6275 Hz.

The control program was designed to log 40 sets of spectral data on each track of the cartridges, allowing up to 10 days data per cartridge. However, a fault in the system resulted in the tape not being rewound at the end of each track so that overwriting of data occurred after a period of about 5 days. This fault, despite a number of visits to the field station, proved impossible to diagnose since the recording cycle takes such a long time to repeat. It was, therefore, decided to change the tape cartridges at 4 day intervals. Even then, some data losses occurred due to:

- (a) power losses at the coastguard lookout, which caused the tape to rewind to Beginning of Tape and then to overwrite data,
- (b) illness or absence of the HMCG sector officer who cared for the equipment, resulting in tapes being changed too late after overwriting had occurred.

A total of 109 tapes were used during the period reported upon.

### 3.5 Data translation and transfer to IBM

The tapes together with HP85B diagnostic printouts were mailed in Jiffy bags to IOSDL where they were processed as follows:

(a) The HP85B printouts were cut into lengths covering periods of one day. These were then stapled in a rough log book allowing one double sided page per day. The other page side was used to enter details regarding tape translation, problems, etc. The diagnostic printouts contained, normally, the TIME message, a single MONITOR message and the LOG message. This allowed a check on buoy battery voltage, spot data values (showing if any channel was inoperative) and quality check data. (The coastguards also found the r.m.s. wave height printout useful and produced a table relating the readings to sea state).

(b) The tape cartridge was replayed, via an Acorn BBC microcomputer using a semi-automatic machine code program (TD), onto floppy disk files; each 1½ hourly set of data was transferred to a separate, consecutively labelled file (e.g. CR3566). A total of 6844 files were created over the period reported upon; each error-free file was 6804 bytes long. Due to the overwrite problem, some files were truncated and these were not used for further processing. Some files required editing due to the overwrite problem. Since they were ASCII files, this could be done conveniently using the standard word processing package "Wordwise Plus". However, since "Wordwise Plus" replaces all line feed characters with pad characters, it was necessary to run a simple program "LFINS" on the edited files to restore the original CR-LF line termination. Another form of editing was required when the real time clock backup battery in the DIREC receiver failed; this resulted in erroneous dates/times in the record headers after a receiving station power failure. Since a large number of records were affected before this could be corrected, a simple program "DATMOD" was written to allow correction of the headers without going through the relatively slow word processor editing technique. On 22-9-1986, a change was made to the advanced disc filing system (ADFS) to allow use of a Winchester disk drive which reduced data file handling time considerably; however this necessitated some minor rewriting of the software.

(c) A number of programs were written to extract and display information from the files, these included:

- PARAMS - prints out computed Date, Time,  $h_s$ ,  $T_p$ ,  $\theta_1(T_p)$ ,  $E_{max}$ ,  $\theta_2(T_p)$  for selected list of consecutive records
- MOD - plots  $E(C_{11})$ ,  $\theta_1$  and  $\theta_2$  and prints out a screen dump for a selected list of records
- WAVSER - plots a time history of up to 16 (one day's) consecutive selected energy spectra with adjustable scaling

(d) After each field tape had been translated and any necessary file editing had been carried out, a proportion, or all of the files were plotted and/or parameterised summary information produced. This allowed an initial check on data quality, in conjunction with the LOG message indicators as mentioned in (a) above. The data was then merged into dayfiles prior to transfer to the IBM mainframe. This was carried out using the program "MAIN4". Where data was missing, dummy data from the file "DUMFILE" was substituted. Where the value of  $H_{rms2}$  was available from the HP85B printout this was inserted in the appropriate position of the dummy file format, otherwise 0000 was inserted. The dayfile names were of the form CYYMMDD

where YY = year e.g. (19)86

MM = month e.g. 07

DD = day e.g. 23.

After a series of dayfiles had been accumulated in the DAYFILES directory, these were transferred to the IBM mainframe using the KERMIT file transfer system over the JANET network. This could be left running overnight, since each dayfile transfer took between 20 and 35 minutes depending upon the usage of the network. The files were then translated to the MIAS format for directional wave data, using the nominal magnetic variation for the buoy site for translation of the magnetically oriented data to true heading referenced data.

### 3.6 Calibrations

The two buoys used for the measurements were calibrated in accordance with conditions specified in the contract. HR Ltd had installed a rotating arm test

rig, manufactured to the Datawell design, for calibration of the heave sensor. This allowed measurement of heave over a wide range of orbital periods down to a minimum of about 4 seconds. The orbit diameter was 1.8 metres. The buoy canister, fitted with a short dummy antenna, was swung in a cradle on the rotating beam. Transmitted signals were initially received on a portable test set constructed by IOS. This test set, which used rechargeable batteries, provided an LCD hexadecimal readout of any selected data channel. It also provided a parallel digital output which could be connected to the BBC microcomputer user port. Programs were written for the BBC to allow full screen display of all data channels, in real-time, as well as logging of a selected number of samples to floppy disk. The latter form of data could then be analysed to obtain the r.m.s. and hence the peak "waveheight" or, in the case of long period orbits, the peak to peak displacement could simply be read off with sufficient accuracy. In estimating the mean calibration from a set of measurements at different periods, the nominal integrator filter correction factor was used. Later calibrations were carried out using a DIREC receiver, HP85B computer and Datawell software procured by HR Ltd at their own expense. See Appendix A.3 Tables 1A and 2A.

Pitch and roll calibrations were carried out using a tilting rig at  $-90^\circ$ ,  $0^\circ$  and  $+90^\circ$  angles in each axis, using a spirit level for setting the angles. Readings were taken off the test set or BBC display. See Appendix A.3 Tables 1B, 1C, 2B and 2C.

Magnetometer calibrations were carried out using a compass table with pneumatically-controlled remote rotation mechanism, with detents at  $10^\circ$  intervals. Readings were again taken using the test set.

All calibrations were recorded in the operations log book. Pitch, roll and heave calibrations were within  $\pm 1.1\%$  of the nominal values on all occasions (usually within  $\pm \frac{1}{2}\%$ ).

The magnetometer readings were initially used to derive a buoy heading using  $\tan^{-1}((2048 - H_y)/(2048 - H_x))$ . However, this showed variations typically of the order of  $\pm 1^\circ$ . The angle of magnetic dip was then calculated, assuming zero pitch and roll angles, and was found to vary more or less

sinusoidally over the 360° rotation. This could be explained by offsets in pitch and roll (not measured during the rotation process) due to the canister not being perfectly level on the rotating table. If, for example, the minimum angle of dip was  $\Theta - \epsilon$ , at a table azimuth angle of  $\varphi$ , and was  $\Theta + \epsilon$ , at a table azimuth angle of  $\varphi + 180$ , then the values of  $p$  and  $r$  required to produce the dip variation are given by

$$\begin{aligned} p &= \epsilon \cos \varphi \\ r &= -\epsilon \sin \varphi \end{aligned}$$

These values were then used to compute the indicated buoy azimuth  $\psi$  from

$$\tan \psi = \frac{(Hy+rHz)(1+\sqrt{1-p^2-r^2})+r(pHx-rHy)}{(Hx-pHz)(1+\sqrt{1-p^2-r^2})-p(pHx-rHy)}$$

(ref. Wavec Manual p.2)

The mean and standard deviation of the difference between the computed  $\psi$  and nominal table azimuth were also computed. See Appendix A.3 Tables 1D and 2D.

The small standard deviations give confidence in the validity of the measurements/correction technique. The mean values are probably partly due to error in setting up the canister on the table, which was done by adjusting the canister azimuth for "zero"  $H_y$ . The errors are, in any case, considered to be insignificant.

The nominal calibrations were used for all data banked since it is not, in any case, possible to correct the slope data for errors in pitch, roll and magnetometer calibrations unless the raw data are logged; to do this would have presented considerable data storage and processing problems.

### 3.7 Accuracy of Measurements

The estimation of the accuracy of directional data obtained with a pitch-roll buoy is more complex than that of one dimensional data obtained with a Waverider buoy; even that is a far from straightforward problem. It is clearly possible to define not only the calibration of the sensors (heave, pitch, roll and magnetometers) but also some of their expected deficiencies -

sensitivity to horizontal acceleration, for example, in the case of the heave, pitch and roll sensors. It is also possible to define the response of the buoy in heave, pitch and roll with a fair degree of confidence. What is less easily defined is the combined response of the buoy and its mooring to waves and currents. Due to the finite spring rate of the mooring, the buoy is restrained from following water particle motion other than in an approximate short term manner. In a regular swell, the buoy will travel downwave until the mean mooring tension matches the mean force on the buoy due to wave motion. Where waves occur in groups one might expect the mean distance of the buoy downwave to increase with the peak of the group and to decrease with the minimum of the group. It would therefore experience horizontal motion with a long period inversely related to the width of the wave spectrum. Such long period motions could possibly upset the long period accelerometer suspension, but no observations of this have been made, as far as is known.

The buoy transfer function in heave  $T_{BH}$  and in pitch or roll  $T_{BP}$  has given by Rademakers (1987), in the form

$$T_{BH} = G_H \cdot \frac{N_H}{D}$$
$$T_{BP} = G_P \cdot \frac{N_P}{D}$$

where  $G$  is a complicated function of the buoy dimensions and of the wavelength involving Bessel functions and exponentials. It is an expression of the buoyancy forces experienced by the various components of the buoy hull.  $N$  and  $D$  are simpler polynomials dealing with, respectively, water particle motions and motions of the buoy.  $N$  is a function of the ratio of wave frequency to the buoy natural frequency (0.61 Hz natural heave frequency, 0.72 Hz natural pitch/roll frequency), of the damping and of the ratio of added mass to total mass (in the case of  $N_H$ ), and of the ratio of added moment of inertia to total moment of inertia (in the case of  $N_P$ ).  $D$  is a function of the ratio of the wave encounter frequency (due to current of speed  $\Delta v$  advecting the waves) to the buoy natural frequency and of the damping. The heave transfer function is essentially flat (equal to unity) for wave frequencies up to 0.35 Hz, thereafter falling off gradually (90% at 0.5 Hz, 64% at 0.6 Hz) when there is no advection of the waves. When the waves are advected by a current in the



direction of propagation of the waves, the wave encounter frequency rises so that at high currents the natural frequencies of the buoy result in increased responses  $T_{BH}$  and (especially)  $T_{BP}$ . When the waves are advected by a current in the opposite direction to the wave direction of propagation, the encounter frequency falls with the result that  $T_{BH}$  and  $T_{BP}$  fall off more slowly with frequency. Results are summarised in the tables; it should be noted that the frequency refers to the wave frequency that would be observed by an observer moving with the stated current. Thus, to obtain the "true spectrum" one has to first correct the spectrum measured at a fixed point for Doppler shift, using

$$\text{"True" } \omega = \frac{2\omega_e}{\sqrt{1 + \frac{4\omega_e \Delta v}{g}} + 1} \quad (\text{where } \omega_e = \text{angular encounter frequency})$$

$$\text{and "True" Spectral Density } S(\omega) = \sqrt{1 + \frac{4\omega_e \Delta v}{g}} \cdot S(\omega_e)$$

(where  $S(\omega_e)$  = measured spectral density at  $\omega_e$ ).

The resulting "True" spectral density must then be multiplied by  $1/T_{B(H \text{ or } P)}$  to obtain the real spectrum which would be observed by an observer moving with the current. In practice, for engineering purposes, this may not be the required spectrum. In order to correct the "encounter frequency spectrum" for buoy response, one must first derive the true angular frequency  $\omega$ , for a given encounter frequency spectral estimate at  $\omega_e$ . The response correction is then calculated for this frequency  $\omega$  and this is then used to correct the estimate at  $\omega_e$ . In order to achieve this, knowledge of the current vector is required and, even then, it is not possible to correct the derived directional parameters.

#### 4. ANALYSIS AND RESULTS

In this report both tabular and graphical information are presented for users. The recommendations proposed by Ewing (1986) for the presentation of directional wave data are followed. Many questions on directionality are comparatively straightforward and should be answerable by direct reference to the tables and figures in this report. Other more complicated questions may require access to the full data set held by the Marine Information and Advisory Service (MIAS) on magnetic tape.

##### 4.1 Definition of parameters

The basic non-directional information contained in this report consist of significant wave height,  $h_s (= 4\sqrt{m_0})$ , mean zero-crossing period,  $T_z (= \sqrt{(m_0/m_2)})$  and wave period at the peak of the wave spectrum,  $T_p$ , where  $m_n$  are the moments of the frequency spectrum evaluated over a frequency range from 0.05 Hz to the Nyquist frequency of 0.63 Hz.

The directional characteristics of the waves are described in terms of the mean wave direction,  $\theta_1$  and the directional spread  $\theta_2$  (see Appendix A.2). If the directional distribution is unimodal then, for a narrow angular distribution,  $\theta_2$  is equal to the r.m.s. spread of wave energy about the mean direction. In some situations the directional distribution can be bimodal and more advanced methods are then necessary to resolve the two peak energies (see Long and Hasselmann, 1979, and Lygre and Krogstad, 1986). We do not consider bimodality in this report.

The effect of strong surface currents off Cromer can be seen directly in the modulation of the skew ratio, R (see Appendix A.4). Appendix A.4 contains a discussion on current influences on wave buoy measurements using estimates of the surface current obtained from the fine-mesh model of Flather (1984).

All wave directions in this report are defined as those directions from which the waves are coming; this is in the same sense as the definition of wind direction.

#### 4.2 Sampling variability

Sampling variability in spectral estimates can be calculated following the work of Blackman and Tukey (1959) and, more recently, by Donelan and Pierson (1983). For the variability in the directional parameters we have used Long (1980). Table 4 gives typical values of the standard deviation of significant wave height, peak period, zero-crossing period and for the two directional parameters. Statistical uncertainties depend on the form and shape of the spectrum and its angular distribution as well as the degrees of freedom of spectral estimates; values given in Table 4 should therefore only be used as a guide to the sampling variability.

#### 4.3 Data return

Wave measurements taken at Cromer cover the period from 7 December 1985 to 30 June 1987. Wave records of 30 min. duration were taken every  $1\frac{1}{2}$  hours. The data return for each month is shown in Table 5 for complete records where all directional wave information is available (denoted by d.w.s) and for records where only the significant wave height,  $h_s$ , is available. The graphs shown in Figs. 3(a)-(e) give a good visual indication of missing data sequences.

Table 6 shows the data return by season and for the whole data set. The overall data return for complete directional information is 73%, while for significant wave height only it is 83%.

In the tables and figures which follow the four seasons are defined as:

Winter : December, January, February

Spring : March, April, May

Summer : June, July, August

Autumn : September, October, November

#### 4.4 Distribution and return value of significant wave height

The mean and maximum values of  $h_s$  for individual months are shown in Table 5. There is a clearly defined seasonal variation. Figs. 3(a)-(e) show the individual values of  $h_s$  throughout each month for the whole period of the measurements. The greatest value of  $h_s$  of 4.8 m was obtained during February 1986. These figures allow the identification of storm periods and, as discussed above, missing data sequences.

The 50-year return value of  $h_s$  was obtained by fitting a Fisher-Tippett Type 1 distribution to the values of  $h_s$  as shown in Figure 4. The parameters of the Fisher-Tippett 1 distribution were estimated using the method of moments. A value of 7.6 m was obtained for the 50-year return value at Cromer. This return value should be used with caution since it is based on a short data base of less than 2 years of wave recordings.

#### 4.5 Joint distribution of wave height and period

Figs. 5(a)-(e) show the joint probability of occurrence of significant wave height,  $h_s$ , with mean zero-crossing period,  $T_z$ , for all data and for each season. Numerical values shown are in parts per thousand for bins of 0.5 m in wave height and 0.5 sec in wave period.

In the figures and the tables to follow, values in a particular cell are those values which include the lower bound but do not include the upper bound of the cell. For example, in Fig. 5(a) 73.2 parts per thousand in the cell  $0.5 \leq h_s < 1$  and  $4 \leq T_z < 4.5$ .

Values of  $T_z$  range from 2 sec to 7.5 sec at Cromer. The wave steepness line corresponding to  $2\pi h_s / g T_z^2 = 1/15$  is drawn in the figures; the autumn and winter seasons have the steepest waves.

#### 4.6 Joint distribution of wave height and direction

Tables 7(a)-(e) give the joint probability of occurrence of significant wave height,  $h_s$ , with mean wave direction,  $\theta_1$ , at the spectral peak for all data and for each season. Values are in parts per thousand for bins of 0.5 m in wave height and  $45^\circ$  in wave direction centred about values of  $0^\circ$ ,  $45^\circ$ ,  $90^\circ$ , etc. Most observations, including those for high waves, come from directions between north-west and north-east, as would be expected for this location.

#### 4.7 Joint distribution of wave period and wave direction

Tables 8(a)-(e) give the joint probability distribution of peak wave period,  $T_p$ , with mean wave direction,  $\theta_1$  at  $T_p$ , for all data and for each season. Values are in parts per thousand with a bin size of  $45^\circ$  for centred values of wave direction (see above).

The wave period at the peak of the wave spectrum was obtained from the reciprocal of the peak frequency as determined from the spectral analysis at a resolution of 0.01 Hz. At low frequencies the evenly spaced values of frequency become widely spaced values of period. It was therefore decided to group values of  $T_p$  as follows:-

Range of $T_p$	Bin size (sec)
1.5 - 8	0.5
8 - 13	1
13 - 15	2
15 - 18	3

The longer values of the peak period occur for wave directions from the north-west to the north-east and for winter and autumn. The most commonly occurring values of  $T_p$  are in the range 4-7 sec.

#### 4.8 Joint distribution of wave height, period and direction

Figs. 6(a)-(e) show the joint probability of occurrence for all three parameters  $h_s$ ,  $T_p$  and  $\Theta_1(T_p)$  for all data and for each season. The numbers inside each circle give the probability of occurrence in parts per ten-thousand for a given combination of  $h_s$  and  $T_p$  (in bins of 0.5 m and, as described above, for  $T_p$ ). For all such observations a directional rose (with values at 45° intervals) gives the direction from which the waves are coming as percentage values. It is important to note the change in the period scale which occurs at 8 sec, 13 sec and 15 sec.

The longer wave periods clearly come from the north. The highest wave heights are for periods in the range 9-12 sec and from directions between north-west and north-east. There are important seasonal differences in the occurrence of high wave heights and long wave periods.

#### 4.9 Distribution of directional spread parameter

In some engineering studies it is important to have information on the directional spread parameter  $\Theta_2$  as well as statistics of mean wave direction. Tables 9(a)-(c) give the joint probability of occurrence of wave height, wave period and wave direction all with directional spread for the whole data set. The most common values of  $\Theta_2$  ( $T_p$ ) are in the range  $20^\circ$ - $30^\circ$  with a tendency for the narrower spreads to be associated with northerly wave directions and long wave periods. High wave heights are usually combined with narrow directional spread.

#### 5. ACKNOWLEDGEMENTS

This work was funded by the Department of Energy.

We thank our colleagues for help during the deployment of the buoy and data collection at Cromer. In particular Messrs C.B. Walters, S. Hanley and S.J. Hearn of Hydraulics Research Limited carried out the deployment, recovery, maintenance and operation of the Wavec buoys. Mr I.M. Fairbairn (HMCG sector officer at Cromer) looked after the receiving station, returned field data tapes to IOSDL and provided access for service visits. Mr E.G. Pitt supplied programs to convert the measured cross-spectra in magnetic co-ordinates to cross-spectra with respect to true north-east co-ordinates. Mr S. Bacon provided plots of the time series of wave height and extreme value estimates. Dr R.A. Flather of the Proudman Oceanographic Laboratory computed the currents off Cromer using his fine-mesh model. Dr A.R. Tabor supplied programs to access the data base of directional spectra held by MIAS.

## 6. REFERENCES

- BLACKMAN, R.B. & TUKEY, J.W. 1958 The measurement of power spectra from the point of view of communications engineering.  
New York: Dover Publications Inc., 190pp.
- DONELAN, M. & PIERSON, W.J. 1983 The sampling variability of estimates of spectra of wind-generated waves.  
Journal of Geophysical Research, 88, 4381-4392.
- EWING, J.A. 1986 Presentation and interpretation of directional wave data.  
Underwater Technology, 12, 17-23.
- FLATHER, R.A. 1984 A numerical model investigation of the storm surge of 31 January and 1 February 1953 in the North Sea.  
Quarterly Journal of the Royal Meteorological Society, 110, 591-612.
- INTERGOVERNMENTAL OCEANOGRAPHIC COMMISSION 1987 GF3: a general formatting system for geo-referenced data.  
Intergovernmental Oceanographic Commission Manuals and Guides No. 17, 42pp. + annexes.
- LONG, R.B. 1980 The statistical evaluation of directional spectrum estimates derived from pitch/roll buoy data.  
Journal of Physical Oceanography, 10, 944-952.
- LONG, R.B. & HASSELMANN, K. 1979 A variational technique for extracting directional spectra from multi-component wave data.  
Journal of Physical Oceanography, 9, 373-381.
- LONGUET-HIGGINS, M.S., CARTWRIGHT, D.E. & SMITH, N.D. 1963 Observations of the directional spectrum of sea waves using the motions of a floating buoy.  
pp.111-132 in, Ocean Wave Spectra.  
Englewood Cliffs, N.J.: Prentice-Hall Inc., 357pp.
- LYGRE, A. & KROGSTAD, H.E. 1986 Maximum entropy estimation of the directional distribution in ocean wave spectra.  
Journal of Physical Oceanography, 16, 2052-2060.
- RADEMAKERS, P. 1987 Regarding the effect of currents on buoy transfer functions. (Personal communication)





17th July 1986 Wavec serial no. 22011 deployed using M.V. "Chudleigh" at 1215 GMT. Decca position - red 12.20, purple 55.50. New mooring design used (rope strops replaced by stainless steel chain, 2 x 15 m rubber cords). Buoy position/condition checked by various ships of the Warbler Shipping fleet on the following dates: 2/8/86, 15/8/86, 2/9/86, 22/9/86, 12/10/86, 28/10/86, 18/11/86, 3/12/86.

6th December 1986 Wavec serial no. 22011 picked up by M.V. "Liberty Moon" in vicinity of platform 4829B.

12th December 1986 Wavec serial no. 22011 retrieved from Great Yarmouth by HR Ltd. Condition on return: superficial damage to hull.

8th January 1987 Wavec serial no. 22011 magnetometer component Hz found to be reading off scale; examination of HP85B printout showed this fault to have occurred at 1630 GMT on 6th December 1988. Quality check failures occurred from 1800 GMT onwards. Fault later found to be due to faulty integrated circuit amplifier - may have occurred at time of recovery. There is no reason why this should have resulted unless buoy flashing light was temporarily close to an active transmitting aerial, resulting in surge on power supply.

9th January 1987 Wavec serial no. 22025 fully calibrated.

22nd January 1987 Wavec serial no. 22025 deployed using M.V. "Chudleigh" at 1515 GMT. Decca position - red 12.15, green 46.00, purple 55.50. Buoy position/condition checked by various ships of the Warbler Shipping fleet on the following dates: 13/2/87, 13/3/87, 17/4/87, 8/5/87, 23/5/87, 12/6/87.

21st July 1987 Wavec serial no. 22025 recovered using M.V. "Dawn Flight" at 1400 GMT (in correct position). Condition on recovery: good, apart from tangled rope/chain.

7th August 1987 Wavec serial no. 22025 fully calibrated.

12th August 1987 Wavec serial no. 22011 fully calibrated.

14th August 1987 Wavec serial no. 22011 returned to IOS by HR Ltd.

### List of Mooring Components

1. Buoy
2. Rope strops to Mooring Cross (4 off)  
(replaced by stainless steel chains 17/7/86 onwards)
3. Mooring cross with single eye fixing
4. 2 metre stainless steel ballast chain.
5. 15 m rubber cord with stainless steel terminals fitted with nylon insulator bushes. Parallel safety line. (Two x 15 m stiffer cords used 17/7/86 onwards)
6. 100 m Polyester braidline rope (16 mm)
7. 10 m  $\frac{7}{8}$ " steel chain
8. 12.5 m  $1\frac{3}{8}$ " steel chain
9. 30 kg Bruce Anchor

Stainless steel shackles used down to level of lower rubber cord terminal.  
Galvanised steel shackles used below this level.

## APPENDIX A.2

### Method of analysis and definition of directional parameters

The cross-spectra obtained from the Wavec buoy system are measured with reference to magnetic co-ordinates using a fluxgate compass. These cross-spectra were first transformed to true North-East axes using a value of  $5.3^\circ(W)$  for the magnetic variation at the buoy location.

The transformed cross-spectra were banked on magnetic tape in the GF3 format recommended by the Intergovernmental Oceanographic Commission (1987). All analysed data in the report have been derived from this data base.

Information contained in the MIAS data base of directional spectra consists of the vertical acceleration and surface slopes referred to true north-east axes. If we denote the vertical acceleration (in units of "g") by the subscript 1 and the slopes in the north and east directions by subscripts 2 and 3 respectively, then it can be shown (Longuet-Higgins et al., 1963) that the six cross-spectra derived from a pitch-roll buoy system are given by

$$\begin{aligned}
 C_{11}(f) &= \int_0^{2\pi} (2\pi f)^4 / g^2 F(f, \theta) d\theta, & Q_{12}(f) &= \int_0^{2\pi} k(2\pi f)^2 / g \cos\theta F(f, \theta) d\theta, \\
 C_{22}(f) &= \int_0^{2\pi} k^2 \cos^2\theta F(f, \theta) d\theta, & Q_{13}(f) &= \int_0^{2\pi} k(2\pi f)^2 / g \sin\theta F(f, \theta) d\theta, \\
 C_{33}(f) &= \int_0^{2\pi} k^2 \sin^2\theta F(f, \theta) d\theta, & C_{23}(f) &= \int_0^{2\pi} k^2 \sin\theta \cos\theta F(f, \theta) d\theta,
 \end{aligned}$$

where  $C_{ij}$  and  $Q_{ij}$  are the co- and quadrature spectra of series  $i$  with  $j$ .  $F(f, \theta)$  is the directional wave spectrum with respect to frequency  $f$  and direction of propagation  $\theta$ .  $k$  is the wave number. Only five of the cross-spectra are independent. This allows estimation of the five Fourier coefficients in the expansion of  $F(f, \theta)$ , namely,

$$a_n + ib_n = \frac{1}{\pi} \int_0^{2\pi} e^{in\theta} F(f, \theta) d\theta, \quad n=0,1,2.$$

In the calculations it is convenient to compute the normalised angular harmonics  $A_1 = a_1/a_0$  etc. where  $\pi a_0$  is the one-dimensional spectrum obtained by

integrating  $F(f,\theta)$  over all directions. Thus

$$A_1 = \frac{Q_{12}}{\sqrt{C_{11}(C_{22} + C_{33})}}, \quad B_1 = \frac{Q_{13}}{\sqrt{C_{11}(C_{22} + C_{33})}},$$

$$A_2 = \frac{C_{22} - C_{33}}{C_{22} + C_{33}}, \quad B_2 = \frac{2C_{23}}{C_{22} + C_{33}}.$$

The angular harmonics  $A_n, B_n$ , and the check ratio (see below) are functions of wave frequency but, for convenience, we suppress this variation.

In the above we make use of the relation

$$C_{11}/(C_{22} + C_{33}) = (2\pi f)^4/g^2 k^2 = \tanh^2 kh$$

which is, in effect, the dispersion relation for waves of small amplitude in water of depth  $h$ . The quantity  $R = \frac{1}{\tanh kh} \left( \frac{C_{11}}{C_{22} + C_{33}} \right)^{1/2}$

provides a check on the functioning of the wave buoy system and on the analysis, since  $R$  should be unity (but see Appendix A.4 for the influence of currents on  $R$ ).

The mean wave direction,  $\theta_1$  and directional spread,  $\theta_2$  are obtained from the first-order angular harmonics, namely

$$\theta_1 = \arctan (B_1/A_1)$$

$$\theta_2 = [2/(s + 1)]^{1/2} \text{ where } s = C_1/(1 - C_1) \text{ and } C_1^2 = A_1^2 + B_1^2.$$

For a narrow directional distribution  $\theta_2$  is the r.m.s. spread about the mean wave direction.

**APPENDIX A.3**

**Summarised Calibrations of Wavecs 22011 and 22025**

**Table 1A. Buoy 22011 heave calibrations**

Date	Range of Periods (sec)	Mean Corrected Sensitivity	Std Deviation
21-11-85*	3.9 - 19.5	1.011	0.0074
24- 6-86*	4.0 - 38.4	1.011	0.0037
12- 8-87**	4.1 - 20.0	1.005	0.0018

\* = IOS technique    \*\* Datawell spectral technique

**Table 1B. Buoy 22011 pitch calibrations**

Date	x up 87.5°	x down 87.5°	Mean Sensitivity (sine of angle/digit)
21-11-85	+1977	-1980	0.0005054
	x up 90°	x down 90°	
24- 6-86	+2032	-1981	0.0004984
12- 8-87	+2004	-1996	0.0005000

**Table 1C. Buoy 22011 roll calibrations**

Date	y up 87.5°	y down 87.5°	Mean Sensitivity
21-11-85	+1988	-1979	0.0005037
	y up 90°	y down 90°	
24- 6-86	+2046	-1979	0.0004969
12- 8-87	+2014	-2000	0.0004983

**Table 1D. Buoy 22011 magnetometer calibration (all angles in degrees)**

Date	Uncorrected pk-pk dip angle $2\epsilon$	Table angle for minimum dip $\phi$	Corrections p	Corrections r	Mean Error	Std Devn
21-11-85	1.552	60	+0.388	-0.672	-1.69	0.09
25- 6-86	1.208	110	-0.207	-0.568	-0.70	0.11
12- 8-87	1.404	160	-0.660	-0.240	3.52	0.50

**Table 2A. Buoy 22025 heave calibrations**

Date	Range of periods (sec)	Mean Corrected Sensitivity (cm/digit)	Std Deviation
21-11-85*	4.1-39.0	0.9950	0.0115
25- 6-86*	4.0-19.5	0.9947	0.0065
9- 1-87**	4.1-25.0	0.9917	0.0058
7- 8-87**	4.1-20.0	0.9961	0.0011

\* = IOS technique      \*\*Datawell spectral technique

**Table 2B. Buoy 22025 pitch calibrations**

Date	x up 87.5°	x down 87.5°	Mean Sensitivity (sine of angle/digit)
21-11-85	+1992	-1990	0.0005023
	x up 90°	x down 90°	
25- 6-86	+1988	-1999	0.0005016
9- 1-87	+1982	-1997	0.0005026
7- 8-87	+2014	-1994	0.0004990

**Table 2C. Buoy 22025 roll calibrations**

Date	y up 87.5°	y down 87.5°	Mean Sensitivity (sine of angle/digit)
21-11-86	+2000	-1998	0.0004998
	y up 90°	y down 90°	
25- 6-86	+2015	-1973	0.0005015
9- 1-87	+2004	-1982	0.0005018
7- 8-87	+2020	-1998	0.0004978

**Table 2D. Buoy 22025 magnetometer calibration**  
(all angles in degrees)

Date	Uncorrected pk-pk dip angle $2\varepsilon$	Table angle for min. dip $\varphi$	Corrections p      r		Mean Error	Std Devn
21-11-85	1.286	130	-0.413	-0.492	-0.93	0.15
25- 6-86	0.939	10	+0.462	-0.0815	-5.50	0.20
9- 1-87	0.959	335	+0.435	+0.203	+4.84	0.17
7- 8-87	0.942	155	-0.427	-0.199	-0.31	0.09

#### APPENDIX A.4

##### Influence of currents on the check ratio

In the absence of currents the check ratio, R (see Appendix A.2), from an ideal moored, surface-following, pitch-roll buoy is unity. In effect the check ratio is a measure of the validity of the linear dispersion relation for waves of small amplitude and of the relative heave and slope response of the buoy.

When a surface current is present the check ratio becomes

$$R(f) = (1 + U \cos\phi/c)^2$$

where U is the magnitude of the current, c is the phase velocity of the waves and  $\phi$  the angle between wave and current directions ( $\phi = 0$  when the current directly opposes the waves).

The check ratio was calculated from the above relation using surface current information from the fine-mesh model of Flather (1984) at the nearest grid point (53°04'N, 1°30'E) to the Wavec buoy location. For every wave record during January 1986, the speed U and angle  $\phi$  were computed and the check ratio evaluated for a wave frequency of 0.275 Hz ( $c = 5.7$  m/sec).

Observed values of the check ratio were averaged over a frequency band from 0.25 Hz to 0.30 Hz to reduce sampling variability. Figure 7 compares the calculated and observed check ratios. The observed modulation of the check ratio is clearly due to the semi-diurnal nature of the tidal currents: the magnitude of the variability in R is also accounted for by surface currents.

**Table 3A. Heave and pitch responses with zero current**

Freq. (Hz)	H Resp.	H Phase	P Resp.	P Phase	H/P Ratio	H/P Phase
0.100	1.000	-0.036	1.001	-0.013	0.999	-0.022
0.200	0.997	-0.325	1.003	-0.118	0.995	-0.207
0.300	0.990	-1.367	1.005	-0.469	0.985	-0.898
0.400	0.970	-4.512	1.007	-1.444	0.963	-3.067
0.500	0.902	-13.507	1.019	-4.182	0.885	-9.325
0.600	0.641	-31.666	1.065	-13.204	0.602	-18.462
0.700	0.281	-39.803	0.997	-48.211	0.281	8.408
0.800	0.089	-31.486	0.304	-87.062	0.293	55.576
0.900	0.009	157.668	0.066	-70.137	0.140	227.805

**Table 3B. Heave and pitch responses with current = 0.500 m/s  
(in direction of wave travel)**

Freq. (Hz)	H Resp.	H Phase	P Resp.	P Phase	H/P Ratio	H/P Phase
0.100	1.001	-0.184	1.002	-0.073	0.999	-0.110
0.200	1.011	-1.080	1.014	-0.407	0.998	-0.672
0.300	1.043	-3.992	1.047	-1.384	0.996	-2.609
0.400	1.107	-13.504	1.136	-4.237	0.974	-9.266
0.500	1.012	-42.387	1.398	-14.613	0.724	-27.775
0.600	0.441	-70.955	1.721	-68.603	0.256	-2.351
0.700	0.147	-65.263	0.450	-120.024	0.327	54.761
0.800	0.045	-47.512	0.104	-115.417	0.429	67.905
0.900	0.005	146.289	0.025	-83.758	0.180	230.048

**Table 3C. Heave and pitch responses with current = -0.500 m/s  
(in opposite direction to wave travel)**

Freq. (Hz)	H Resp.	H Phase	P Resp.	P Phase	H/P Ratio	H/P Phase
0.100	0.998	0.111	1.000	0.046	0.998	0.065
0.200	0.985	0.401	0.993	0.164	0.992	0.237
0.300	0.946	0.927	0.969	0.353	0.976	0.573
0.400	0.865	1.983	0.915	0.675	0.945	1.308
0.500	0.732	4.377	0.819	1.302	0.894	3.075
0.600	0.557	9.756	0.671	2.713	0.830	7.043
0.700	0.377	18.605	0.480	6.312	0.784	12.294
0.800	0.187	25.124	0.283	16.381	0.660	8.742
0.900	0.026	-154.169	0.143	40.086	0.178	-194.255



**Table 3D. Heave and pitch responses with current = 1.000 m/s  
(in direction of wave travel)**

Freq. (Hz)	H Resp.	H Phase	P Resp.	P Phase	H/P Ratio	H/P Phase
0.100	1.003	-0.332	1.003	-0.134	0.999	-0.198
0.200	1.026	-1.866	1.025	-0.706	1.001	-1.160
0.300	1.105	-7.040	1.097	-2.413	1.007	-4.627
0.400	1.265	-26.258	1.320	-8.142	0.958	-18.117
0.500	0.860	-74.056	2.128	-39.544	0.404	-34.512
0.600	0.273	-89.893	0.909	-124.207	0.300	34.314
0.700	0.089	-75.323	0.215	-134.779	0.414	59.455
0.800	0.027	-54.030	0.056	-121.960	0.487	67.930
0.900	0.003	141.472	0.014	-87.782	0.195	229.255

**Table 3E. Heave and pitch responses with current = -1.000 m/s  
(in opposite direction to wave travel)**

Freq. (Hz)	H Resp.	H Phase	P Resp.	P Phase	H/P Ratio	H/P Phase
0.100	0.997	0.258	0.998	0.106	0.998	0.151
0.200	0.973	1.101	0.984	0.437	0.989	0.664
0.300	0.908	2.959	0.939	1.102	0.968	1.857
0.400	0.786	6.874	0.848	2.361	0.927	4.513
0.500	0.610	14.954	0.702	4.728	0.869	10.226
0.600	0.416	30.678	0.510	9.217	0.816	21.461
0.700	0.258	55.823	0.308	18.062	0.837	37.762
0.800	0.126	82.702	0.145	36.797	0.874	45.905
0.900	0.019	-76.998	0.057	74.296	0.328	-151.295

**Table 4**  
**Uncertainties associated with sampling variability**  
**Degrees of freedom = 36**

Variable	Standard deviation
$h_s$	3%-5% of $h_s$
$T_p, T_z$	approx. 5% of $T_p, T_z$
$\Theta_1(T_p)$	3°-7°
$\Theta_2(T_p)$	3°-6°
$R(T_p)$	±0.07

**Table 5**  
**Cromer Wavec Buoy**  
**Data return and mean and maximum  $h_s$  by month**

Month	% data return $h_s$ d.w.s.		$h_s$ (m) mean max.	
Dec. 1985	81	64	1.14	3.91
Jan. 1986	99	96	1.81	4.53
Feb. "	99	72	1.85	4.81
Mar. "	99	96	0.93	4.32
Apr. "	99	99	1.09	4.32
May "	99	99	0.71	1.73
June "	59	59	0.97	3.36
July "	46	46	0.71	2.02
Aug. "	96	66	1.09	3.44
Sept. "	99	96	0.93	3.32
Oct. "	99	91	0.95	3.14
Nov. "	98	66	1.15	3.72
Dec. "	18	15	1.25	2.03
Jan. 1987	30	27	1.03	2.15
Feb. "	99	95	0.97	2.39
Mar. "	84	67	1.36	4.28
Apr. "	97	91	0.73	2.90
May "	94	91	1.14	3.75
June "	93	54	0.74	2.04
All data	83%	73%		

**Table 6**  
**Cromer Wavec Buoy**  
**Data return by season and year**

Season	Number of records		% data return	
	$h_s$	d.w.s.	$h_s$	d.w.s.
Winter (Dec-Feb)	2023	1748	70	61
Spring (Mar-May)	2805	2664	95	90
Summer (June-Aug)	1432	1100	73	56
Autumn (Sept-Nov)	1435	1227	99	84
All data	7695	6739	83	73

Wave direction,  $\theta_1(T_p)$ : deg; central value

Table 7(a): All data  
Wave height,  $h_s$  (m)

	0-0.5	0.5-1.0	1.0-1.5	1.5-2.0	2.0-2.5	2.5-3.0	3.0-3.5	3.5-4.0	4.0-4.5	4.5-5.0	
0	55.8	139.0	77.2	33.5	16.2	11.1	7.4	2.2	0.6	0.1	343.4
45	25.5	47.6	22.3	14.2	15.0	12.3	7.0	4.0	1.8	0.3	150.2
90	39.5	41.4	15.9	6.2	7.6	3.9	1.3	0.3	0.1	-	116.4
135	33.4	47.2	22.9	7.0	1.6	0.1	-	-	-	-	112.2
180	5.2	11.0	10.8	1.8	-	-	-	-	-	-	28.7
225	4.9	17.1	10.8	3.4	0.1	0.1	0.1	-	-	-	36.6
270	12.6	44.7	52.4	13.5	3.6	1.6	0.3	-	-	-	128.5
315	10.4	29.2	22.3	10.4	5.8	3.4	1.5	1.0	0.3	-	84.2
Totals	187.3	377.2	234.5	90.1	49.9	32.6	17.7	7.6	2.8	0.4	1000

**Table 7(b): Winter  
Wave height,  $h_s$  (m)**

	0-0.5	0.5-1.0	1.0-1.5	1.5-2.0	2.0-2.5	2.5-3.0	3.0-3.5	3.5-4.0	4.0-4.5	4.5-5.0	
0	29.7	103.5	107.6	42.9	20.0	5.1	5.7	5.1	1.1	0.6	321.4
45	8.0	48.6	45.8	32.6	40.6	22.3	19.5	11.4	6.9	1.1	236.9
90	7.4	32.0	26.9	18.3	20.0	10.9	4.6	0.6	0.6	-	121.3
135	5.1	31.5	24.6	13.7	5.1	0.6	-	-	-	-	80.7
180	2.9	9.2	14.9	1.7	-	-	-	-	-	-	28.7
225	1.1	14.9	13.7	8.6	0.6	-	-	-	-	-	38.9
270	1.1	15.4	55.5	26.3	6.3	1.7	0.6	-	-	-	106.9
315	0.6	12.0	18.9	12.0	10.9	3.4	2.3	4.0	1.1	-	65.2
Totals	56.1	267.2	307.8	156.2	103.5	44.1	32.6	21.2	9.7	1.7	1000

Wave direction,  $\theta_1(T_p)$  : deg; central value

Wave direction,  $\theta_1(T_p)$ : deg; central value

Table 7(c): Spring  
Wave height,  $h_s$  (m)

	0-0.5	0.5-1.0	1.0-1.5	1.5-2.0	2.0-2.5	2.5-3.0	3.0-3.5	3.5-4.0	4.0-4.5	4.5-5.0	
0	69.8	109.6	59.3	23.3	19.5	15.4	8.3	1.9	0.8	-	307.9
45	42.8	60.1	16.9	12.8	11.3	15.8	4.1	2.3	-	-	166.1
90	63.4	54.1	8.6	3.4	6.0	2.6	0.4	0.4	-	-	138.9
135	51.4	65.3	14.6	2.3	0.8	-	-	-	-	-	134.4
180	6.4	12.0	9.0	1.1	-	-	-	-	-	-	28.5
225	8.3	20.6	12.0	0.4	-	0.4	0.4	-	-	-	42.1
270	12.8	49.2	42.0	5.6	3.4	2.6	0.4	-	-	-	116.0
315	5.6	28.9	18.0	6.8	4.9	2.3	-	-	-	-	66.5
Totals	260.5	399.8	180.6	55.6	45.8	39.0	13.5	4.5	0.8	-	1000

Wave direction,  $\theta_1(T^p)$ : deg; central value

Table 7(d): Summer  
Wave height,  $h_s$  (m)

	0-0.5	0.5-1.0	1.0-1.5	1.5-2.0	2.0-2.5	2.5-3.0	3.0-3.5	3.5-4.0	4.0-4.5	4.5-5.0	
0	53.6	206.4	55.5	41.8	16.4	15.5	9.1	-	-	-	398.3
45	28.2	42.7	10.9	4.5	-	-	-	-	-	-	86.3
90	49.1	40.9	18.2	0.9	-	-	-	-	-	-	109.1
135	56.4	43.6	23.6	-	-	-	-	-	-	-	123.6
180	4.5	9.1	10.9	-	-	-	-	-	-	-	24.5
225	4.5	13.6	6.4	0.9	-	-	-	-	-	-	25.4
270	20.0	59.1	37.3	6.4	-	-	-	-	-	-	122.8
315	20.0	46.4	27.3	10.9	3.6	0.9	0.9	-	-	-	110.0
Totals	236.4	461.8	190.0	65.5	20.0	16.4	10.0	-	-	-	1000



Table 7(e): Autumn  
Wave height,  $h_s$  (m)

	0-0.5	0.5-1.0	1.0-1.5	1.5-2.0	2.0-2.5	2.5-3.0	3.0-3.5	3.5-4.0	4.0-4.5	4.5-5.0	
0	64.4	193.2	92.1	35.0	3.3	6.5	6.5	0.8	-	-	401.9
45	10.6	23.6	10.6	-	-	1.6	1.6	0.8	-	-	48.8
90	24.4	27.7	13.9	-	-	-	-	-	-	-	66.0
135	13.9	33.4	37.5	13.9	-	-	-	-	-	-	98.7
180	6.5	13.0	9.0	4.9	-	-	-	-	-	-	33.4
225	3.3	15.5	8.1	4.9	-	-	-	-	-	-	31.8
270	22.0	63.6	83.9	18.7	3.3	0.8	-	-	-	-	192.3
315	26.1	39.1	31.8	15.5	2.4	8.1	4.1	-	-	-	127.1
Totals	171.1	409.1	286.9	92.9	9.0	17.1	12.2	1.6	-	-	1000

Wave direction,  $\theta_1(T_p)$ : deg; central value

Table 8(a): All data  
Wave direction,  $\theta_1$  (Tp): deg; central value

	0	45	90	135	180	225	270	315	
1.5-2.0	-	-	0.3	-	-	-	-	-	0.3
2.0-2.5	-	0.1	0.3	0.9	1.5	0.1	0.3	0.3	3.6
2.5-3.0	1.2	0.4	1.3	5.5	3.0	3.3	4.2	2.1	20.9
3.0-3.5	2.2	1.0	6.2	10.8	4.6	7.3	12.0	3.6	47.8
3.5-4.0	1.6	4.0	14.4	16.0	7.7	10.1	20.8	9.1	83.7
4.0-4.5	5.5	11.3	17.4	19.1	8.6	8.6	28.8	12.6	111.9
4.5-5.0	8.9	10.4	18.1	12.6	2.7	4.7	22.6	11.4	91.4
5.0-5.5	16.2	16.6	21.2	15.6	0.7	2.1	23.0	13.9	109.4
5.5-6.0	13.2	8.5	7.3	6.2	-	0.3	8.8	6.7	50.9
6.0-6.5	42.1	24.9	12.8	12.5	-	-	7.3	14.1	113.7
6.5-7.0	41.0	18.0	5.5	5.6	-	0.1	0.6	5.2	76.0
7.0-7.5	53.4	17.4	6.5	4.7	-	-	0.4	4.0	86.5
7.5-8.0	49.4	15.4	3.7	2.1	-	-	-	1.3	72.0
8 - 9	37.8	9.5	1.0	0.4	-	-	-	-	48.8
9 - 10	23.7	7.9	0.1	-	-	-	-	-	31.8
10 - 11	16.9	3.4	-	-	-	-	-	-	20.3
11 - 12	13.5	0.4	-	-	-	-	-	-	13.9
12 - 13	9.2	0.7	-	-	-	-	-	-	9.9
13 - 15	6.7	-	-	-	-	-	-	-	6.7
15 - 18	0.6	-	-	-	-	-	-	-	0.6
Totals	343.4	150.2	116.4	112.2	28.7	36.6	128.5	84.2	1000

Table 8(b): Winter  
Wave direction,  $\theta_1$  (Tp): deg; central value

	0	45	90	135	180	225	270	315	
1.5-2.0	-	-	-	-	-	-	-	-	-
2.0-2.5	-	-	-	-	-	-	0.6	-	0.6
2.5-3.0	-	-	-	0.6	3.4	1.1	-	-	5.1
3.0-3.5	1.1	-	-	4.0	4.6	5.1	3.4	1.7	20.0
3.5-4.0	-	0.6	0.6	4.6	8.0	7.4	9.2	4.0	34.3
4.0-4.5	2.9	4.6	2.9	14.3	8.0	12.6	21.7	7.4	74.4
4.5-5.0	9.2	10.3	10.3	7.4	4.0	9.7	17.7	3.4	72.1
5.0-5.5	12.0	10.9	20.0	14.3	0.6	2.9	28.0	6.9	95.5
5.5-6.0	10.9	10.3	10.3	5.1	-	-	10.9	8.6	56.1
6.0-6.5	38.3	37.8	29.2	9.2	-	-	14.3	13.2	141.9
6.5-7.0	30.3	38.9	14.9	6.9	-	-	-	9.2	100.1
7.0-7.5	54.3	34.3	17.7	10.9	-	-	1.1	7.4	125.9
7.5-8.0	41.8	34.9	12.6	2.9	-	-	-	3.4	95.5
8 - 9	37.8	20.0	2.3	0.6	-	-	-	-	60.6
9 - 10	25.7	18.9	0.6	-	-	-	-	-	45.2
10 - 11	20.0	13.2	-	-	-	-	-	-	33.2
11 - 12	16.0	1.7	-	-	-	-	-	-	17.7
12 - 13	9.7	0.6	-	-	-	-	-	-	10.3
13 - 15	10.3	-	-	-	-	-	-	-	10.3
15 - 18	1.1	-	-	-	-	-	-	-	1.1
Totals	321.4	236.9	121.3	80.7	28.7	38.9	106.9	65.2	1000

Table 8(c): Spring  
Wave direction,  $\theta_1$  (Tp): deg; central value

	0	45	90	135	180	225	270	315	
1.5-2.0	-	-	0.4	-	-	-	-	-	0.4
2.0-2.5	-	0.4	-	1.5	2.3	-	-	-	4.1
2.5-3.0	0.4	0.4	3.0	7.1	2.6	5.3	3.4	1.9	24.0
3.0-3.5	2.3	2.3	12.4	18.8	6.4	9.4	12.4	1.9	65.7
3.5-4.0	3.0	6.8	29.3	25.2	6.0	14.6	21.8	6.8	113.4
4.0-4.5	5.3	15.8	27.0	24.4	9.0	8.3	29.7	8.6	128.0
4.5-5.0	7.1	8.3	24.0	15.0	1.5	2.3	22.5	10.1	90.8
5.0-5.5	15.8	20.6	18.4	16.9	0.8	1.5	13.9	15.8	103.6
5.5-6.0	13.1	10.9	7.1	6.8	-	0.4	5.6	3.4	47.3
6.0-6.5	43.5	28.5	7.1	10.9	-	-	5.3	12.4	107.7
6.5-7.0	38.3	16.9	3.0	4.9	-	0.4	1.1	2.6	67.2
7.0-7.5	44.7	21.0	4.9	2.6	-	-	0.4	2.3	75.8
7.5-8.0	39.0	15.0	1.1	0.4	-	-	-	0.8	56.3
8 - 9	30.0	10.5	1.1	-	-	-	-	-	41.7
9 - 10	20.6	7.5	-	-	-	-	-	-	28.2
10 - 11	18.0	-	-	-	-	-	-	-	18.0
11 - 12	14.6	-	-	-	-	-	-	-	14.6
12 - 13	8.3	1.1	-	-	-	-	-	-	9.4
13 - 15	3.8	-	-	-	-	-	-	-	3.8
15 - 18	-	-	-	-	-	-	-	-	-
Totals	307.9	166.1	138.9	134.4	28.5	42.1	116.0	66.5	1000

Table 8(d): Summer  
Wave direction,  $\theta_1$  (Tp): deg; central value

	0	45	90	135	180	225	270	315	
1.5-2.0	-	-	0.9	-	-	-	-	-	0.9
2.0-2.5	-	-	0.9	1.8	0.9	-	0.9	1.8	6.4
2.5-3.0	3.6	1.8	0.9	12.7	0.9	0.9	9.1	5.5	35.5
3.0-3.5	4.5	0.9	6.4	6.4	3.6	7.3	12.7	4.5	46.4
3.5-4.0	0.9	5.5	10.9	19.1	10.0	2.7	22.7	13.6	85.5
4.0-4.5	3.6	13.6	20.9	26.4	6.4	5.5	27.3	16.4	120.0
4.5-5.0	5.5	15.5	23.6	15.5	1.8	5.5	24.5	15.5	107.3
5.0-5.5	25.5	20.9	36.4	20.9	0.9	3.6	16.4	22.7	147.3
5.5-6.0	17.3	4.5	2.7	10.9	-	-	6.4	11.8	53.6
6.0-6.5	55.5	15.5	5.5	10.0	-	-	2.7	15.5	104.5
6.5-7.0	61.8	7.3	-	-	-	-	-	0.9	70.0
7.0-7.5	83.6	0.9	-	-	-	-	-	1.8	86.4
7.5-8.0	70.0	-	-	-	-	-	-	-	70.0
8 - 9	49.1	-	-	-	-	-	-	-	49.1
9 - 10	10.9	-	-	-	-	-	-	-	10.9
10 - 11	3.6	-	-	-	-	-	-	-	3.6
11 - 12	2.7	-	-	-	-	-	-	-	2.7
12 - 13	-	-	-	-	-	-	-	-	-
13 - 15	-	-	-	-	-	-	-	-	-
15 - 18	-	-	-	-	-	-	-	-	-
Totals	398.3	86.3	109.1	123.6	24.5	25.4	122.8	110.0	1000

Table 8(e): Autumn  
Wave direction,  $\theta_1$  (Tp): deg; central value

	0	45	90	135	180	225	270	315	
1.5-2.0	-	-	-	-	-	-	-	-	-
2.0-2.5	-	-	0.8	-	2.4	0.8	-	-	4.1
2.5-3.0	2.4	-	-	2.4	4.9	4.1	7.3	2.4	23.6
3.0-3.5	1.6	-	1.6	7.3	1.6	5.7	22.8	9.0	49.7
3.5-4.0	1.6	1.6	4.9	9.8	9.0	10.6	33.4	17.1	88.0
4.0-4.5	11.4	9.0	13.9	8.1	10.6	6.5	38.3	25.3	123.1
4.5-5.0	15.5	10.6	11.4	12.2	4.1	2.4	27.7	22.0	105.9
5.0-5.5	14.7	12.2	15.5	9.8	0.8	0.8	41.6	12.2	107.6
5.5-6.0	13.0	4.1	7.3	2.4	-	0.8	14.7	6.5	48.9
6.0-6.5	32.6	7.3	8.1	22.8	-	-	5.7	17.9	94.5
6.5-7.0	43.2	-	2.4	10.6	-	-	0.8	9.0	66.0
7.0-7.5	44.0	-	-	4.9	-	-	-	4.9	53.8
7.5-8.0	64.4	2.4	-	6.5	-	-	-	0.8	74.2
8 - 9	44.8	0.8	-	1.6	-	-	-	-	47.3
9 - 10	39.1	-	-	-	-	-	-	-	39.1
10 - 11	22.0	-	-	-	-	-	-	-	22.0
11 - 12	17.1	-	-	-	-	-	-	-	17.1
12 - 13	18.7	0.9	-	-	-	-	-	-	19.6
13 - 15	13.9	-	-	-	-	-	-	-	13.9
15 - 18	1.6	-	-	-	-	-	-	-	1.6
Totals	401.9	48.8	66.0	98.7	33.4	31.8	192.3	127.1	1000

Table 9(a)  
Spread parameter,  $\theta_2$  (Tp): deg

	10-20	20-30	30-40	40-50	50-60	60-70	70-80	
Wave height, $h_s$ (m)								
0 - 0.5	0.1	34.4	65.1	43.9	27.3	13.2	3.1	187.3
0.5-1.0	3.6	137.9	143.0	61.9	21.7	7.9	1.3	377.2
1.0-1.5	4.2	101.6	93.8	26.3	6.8	1.8	-	234.5
1.5-2.0	4.5	53.0	26.7	4.0	1.9	-	-	90.1
2.0-2.5	1.6	31.6	15.7	0.7	0.1	-	-	49.9
2.5-3.0	1.2	22.6	8.8	-	0.1	-	-	32.6
3.0-3.5	-	13.2	4.3	0.1	-	-	-	17.7
3.5-4.0	-	4.0	3.6	-	-	-	-	7.6
4.0-4.5	0.1	1.3	1.3	-	-	-	-	2.8
4.5-5.0	-	0.1	0.3	-	-	-	-	0.4
Totals	15.3	399.8	362.7	137.0	58.0	22.9	4.5	1000

Table 9(b)  
Spread parameter,  $\theta_2$  (Tp): deg

	10-20	20-30	30-40	40-50	50-60	60-70	70-80	
1.5-2.0	-	-	-	0.3	-	-	-	0.3
2.0-2.5	-	0.1	1.8	1.0	0.3	0.3	-	3.5
2.5-3.0	-	2.2	7.7	7.7	2.7	0.6	-	20.9
3.0-3.5	0.1	5.2	16.5	14.4	7.7	3.4	0.4	47.8
3.5-4.0	0.3	11.6	32.3	22.3	11.3	4.7	1.2	83.7
4.0-4.5	0.3	18.8	45.1	26.4	13.7	5.5	2.1	111.9
4.5-5.0	0.4	22.4	36.1	20.6	8.8	2.5	0.6	91.4
5.0-5.5	1.0	38.9	42.1	15.4	7.9	3.9	0.1	109.3
5.5-6.0	0.9	21.1	18.5	7.3	1.6	1.5	-	50.9
6.0-6.5	4.5	62.0	38.3	7.3	1.5	0.1	-	113.7
6.5-7.0	3.1	54.5	15.9	1.5	0.9	0.1	-	76.0
7.0-7.5	3.1	62.9	19.4	0.6	0.4	-	-	86.5
7.5-8.0	1.5	50.9	18.5	1.0	-	-	-	72.0
8 - 9	-	30.3	18.3	0.3	-	-	-	48.8
9 - 10	-	12.5	18.4	0.9	-	-	-	81.8
10 - 11	-	4.3	14.1	1.9	-	-	-	20.3
11 - 12	-	0.9	11.0	2.1	-	-	-	13.9
12 - 13	-	0.7	5.6	3.3	0.3	-	-	9.9
13 - 15	-	0.4	2.7	2.5	0.9	0.1	-	6.7
15 - 18	-	-	0.3	0.1	0.1	-	-	0.6
Totals	15.3	399.8	362.7	137.0	58.0	22.9	4.5	1000



Table 9(c)  
Spread parameter,  $\theta_2$  (Tp): deg

Wave direction, $\theta_1$ (Tp): deg; central value	10-20	20-30	30-40	40-50	50-60	60-70	70-80	
0	3.6	175.0	131.9	25.1	5.9	1.8	-	343.3
45	2.8	68.9	50.5	16.2	8.3	2.8	0.6	150.1
90	0.9	36.1	40.1	23.7	11.3	3.9	0.3	116.3
135	5.0	45.0	36.9	13.7	7.7	3.1	0.7	112.1
180	0.1	3.6	11.4	6.5	4.2	1.6	1.3	28.7
225	-	0.6	9.3	13.4	7.3	5.3	0.7	36.6
270	0.9	38.4	52.1	24.6	9.6	2.2	0.7	128.5
315	1.9	32.3	30.4	13.8	3.7	2.1	-	84.2
Totals	15.3	399.8	362.7	137.0	58.0	22.9	4.5	1000

Fig. 3(a)

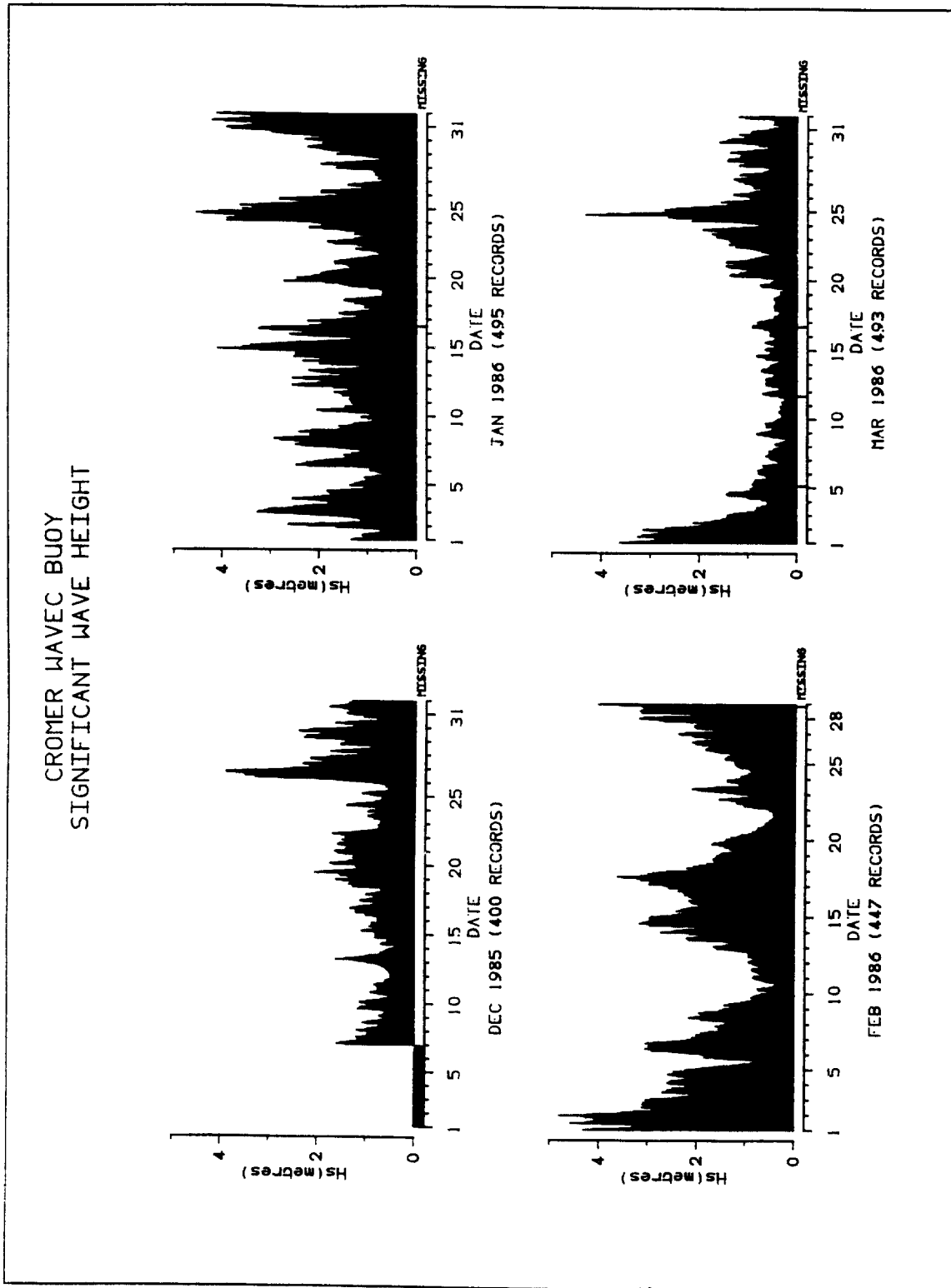


Fig. 3(b)

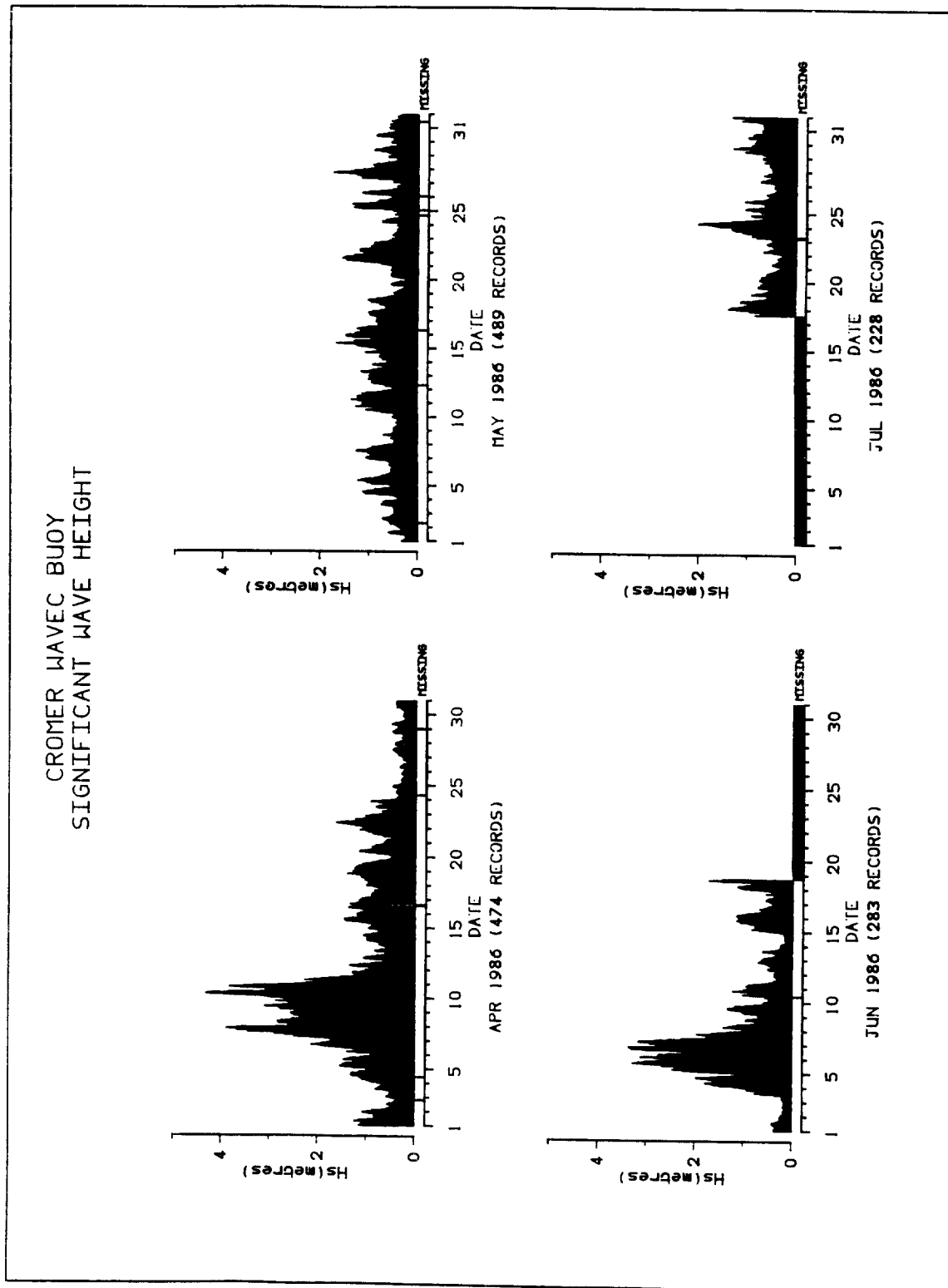
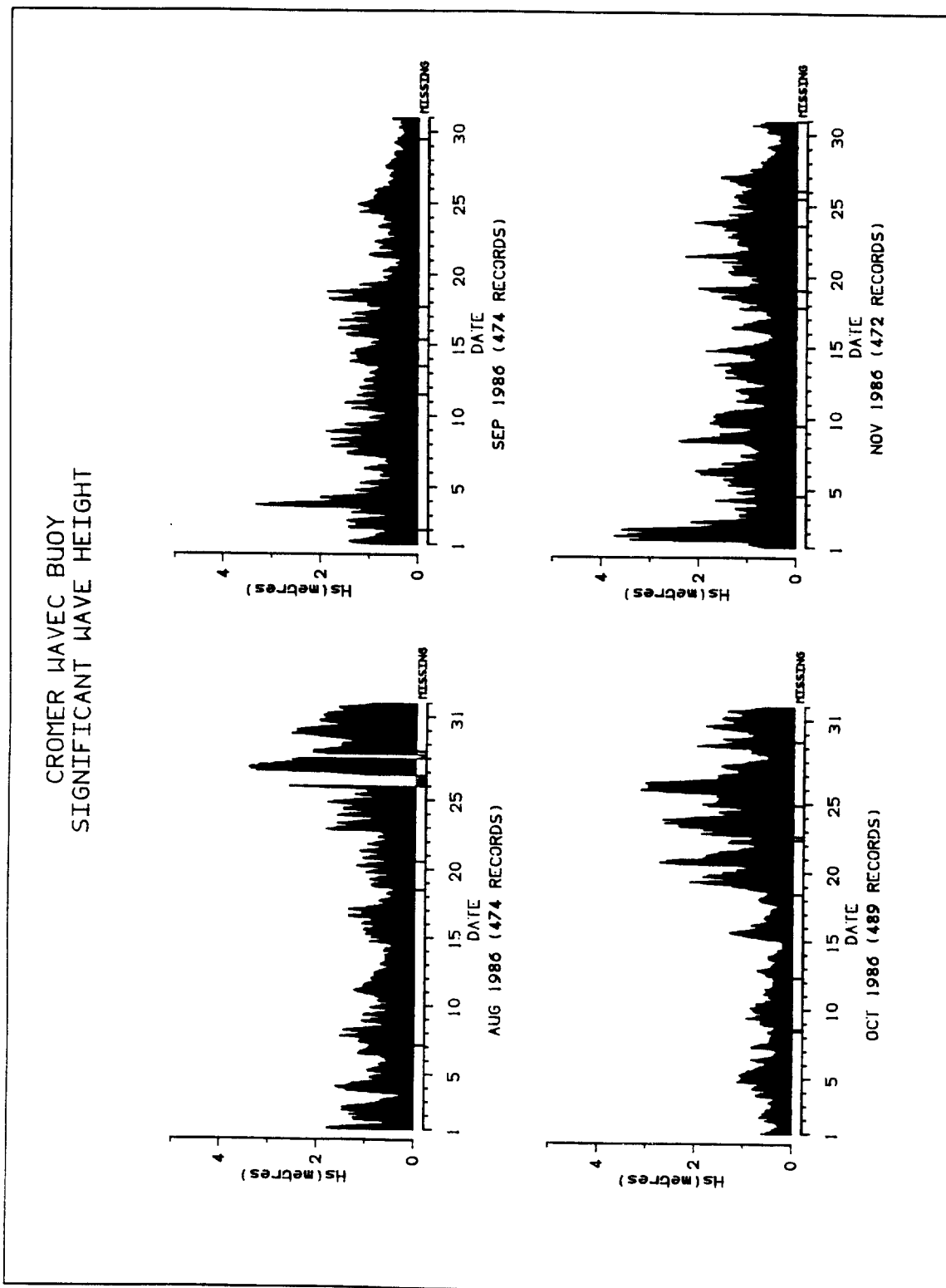


Fig. 3(c)



CROMER WAVEC BUOY  
SIGNIFICANT WAVE HEIGHT

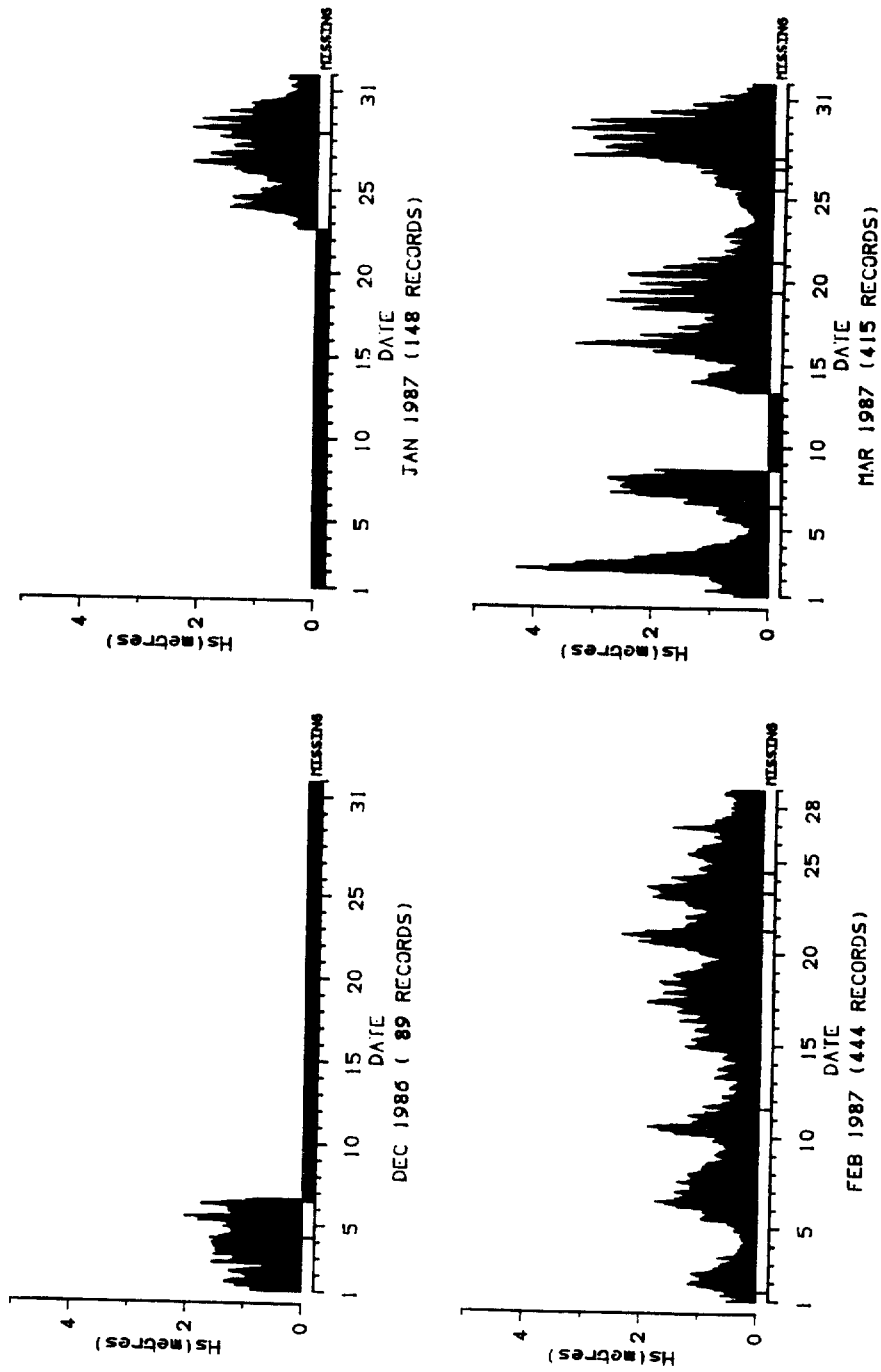
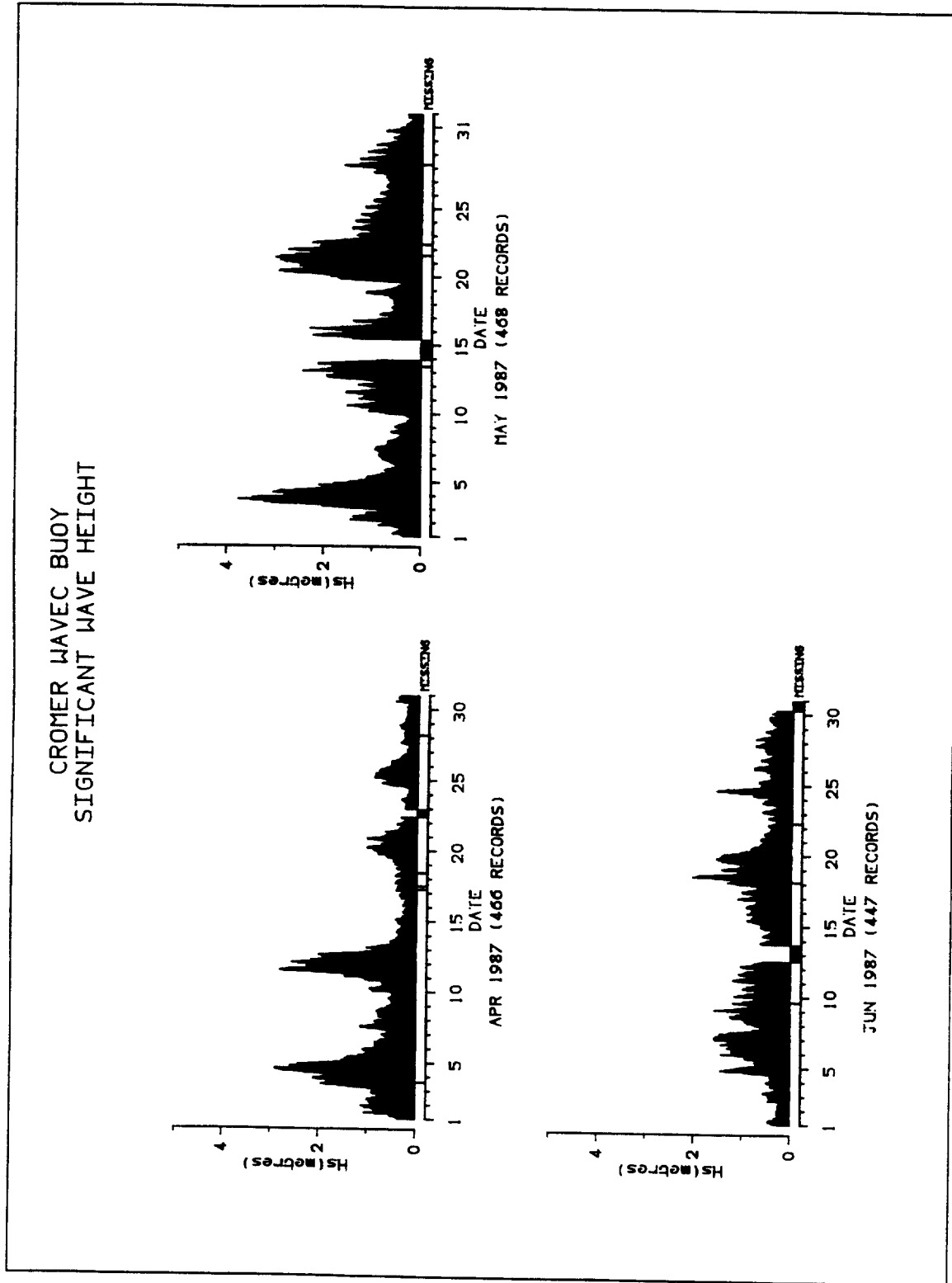


Fig. 3(d)

Fig. 3(e)



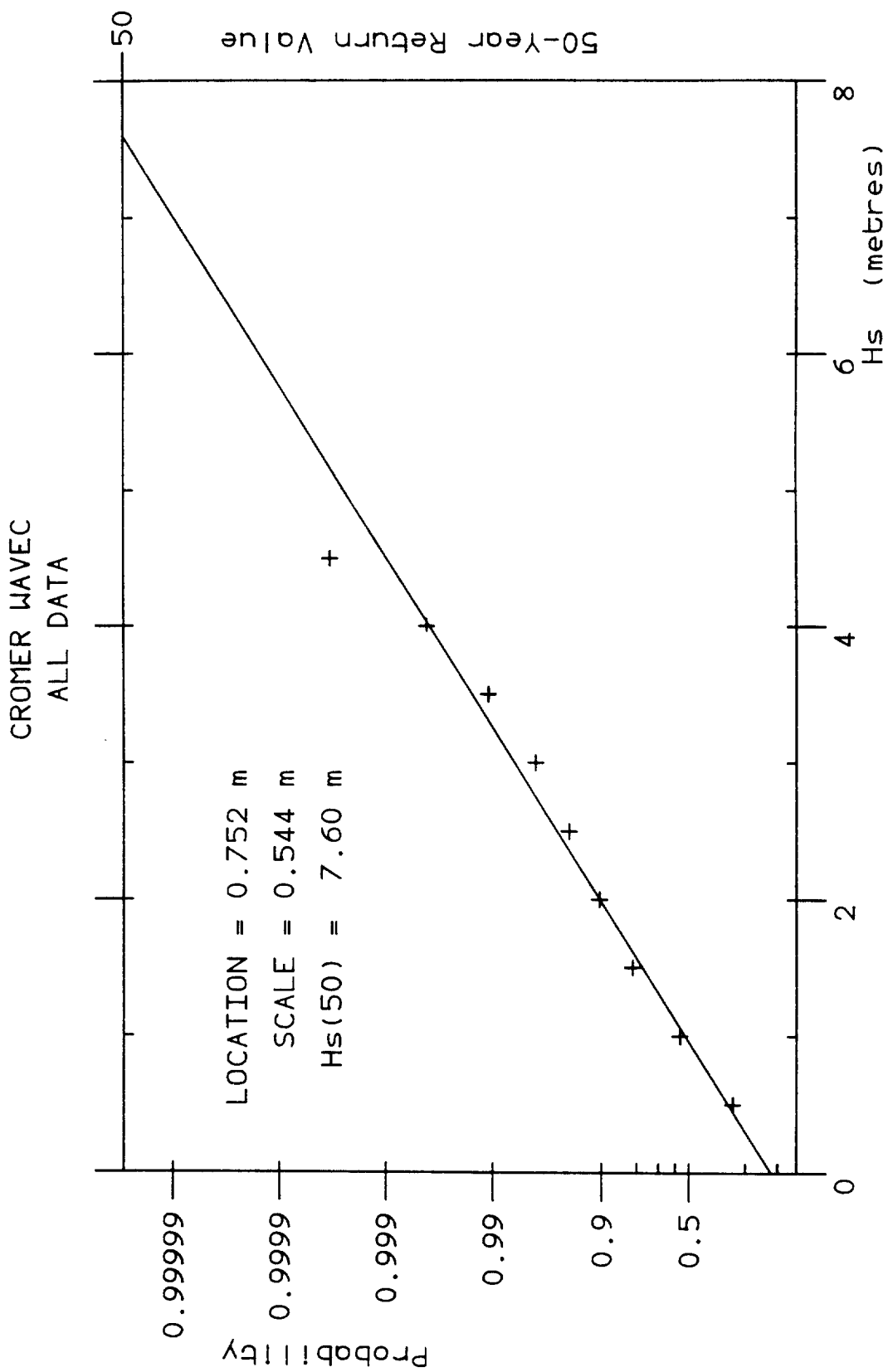


Fig. 4

CUMULATIVE HS PROBABILITY on FT-I SCALE

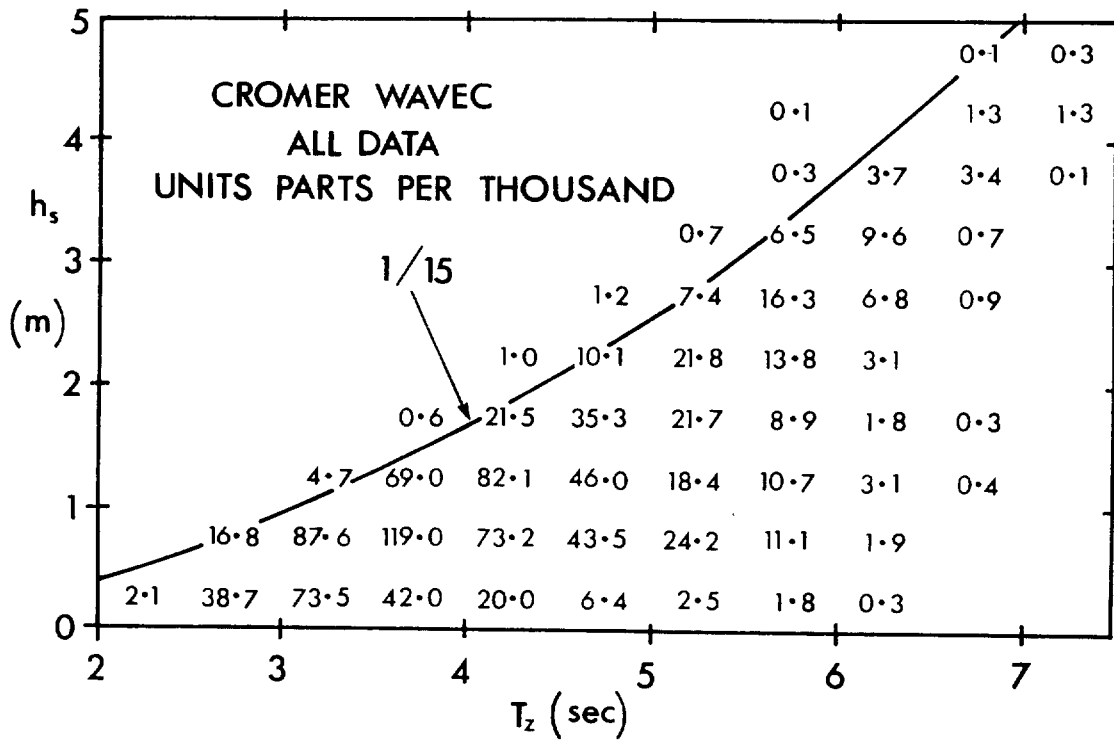


Fig. 5(a)

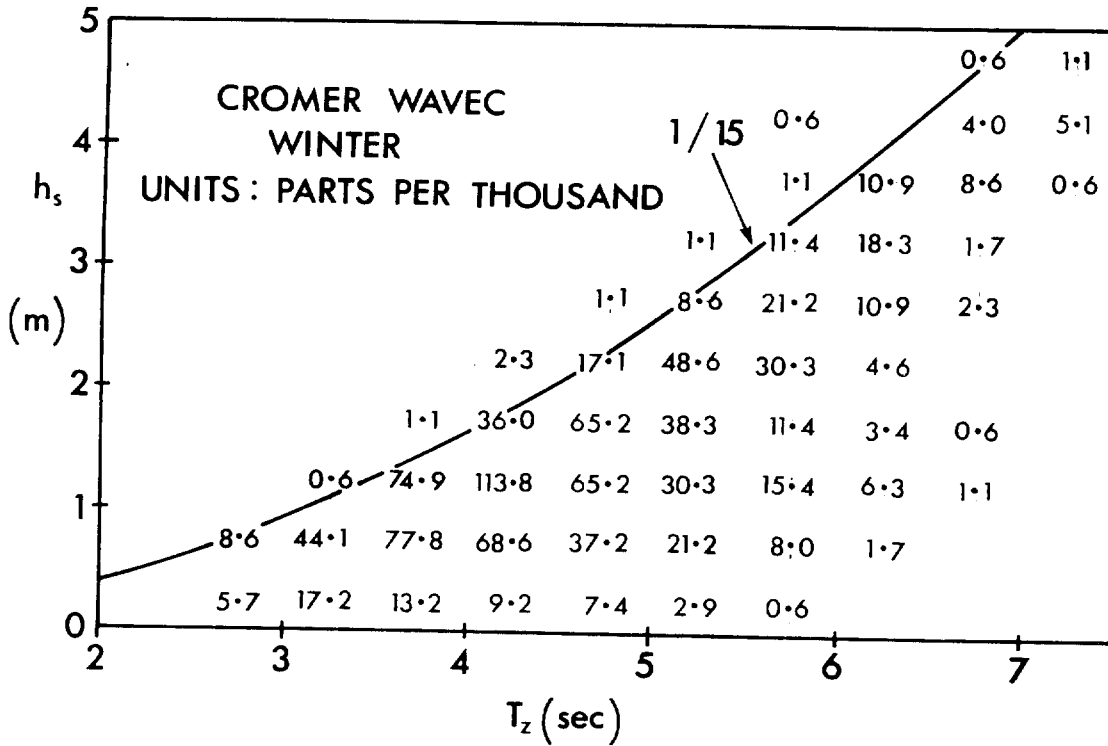


Fig. 5(b)



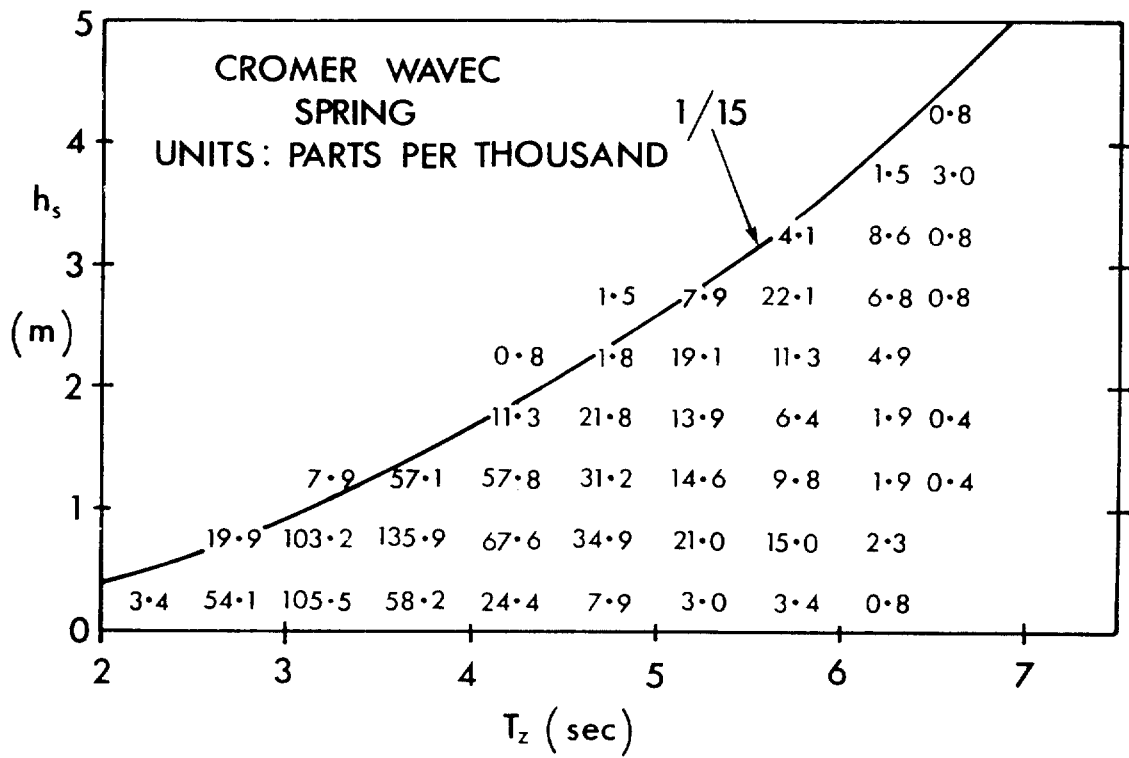


Fig. 5(c)

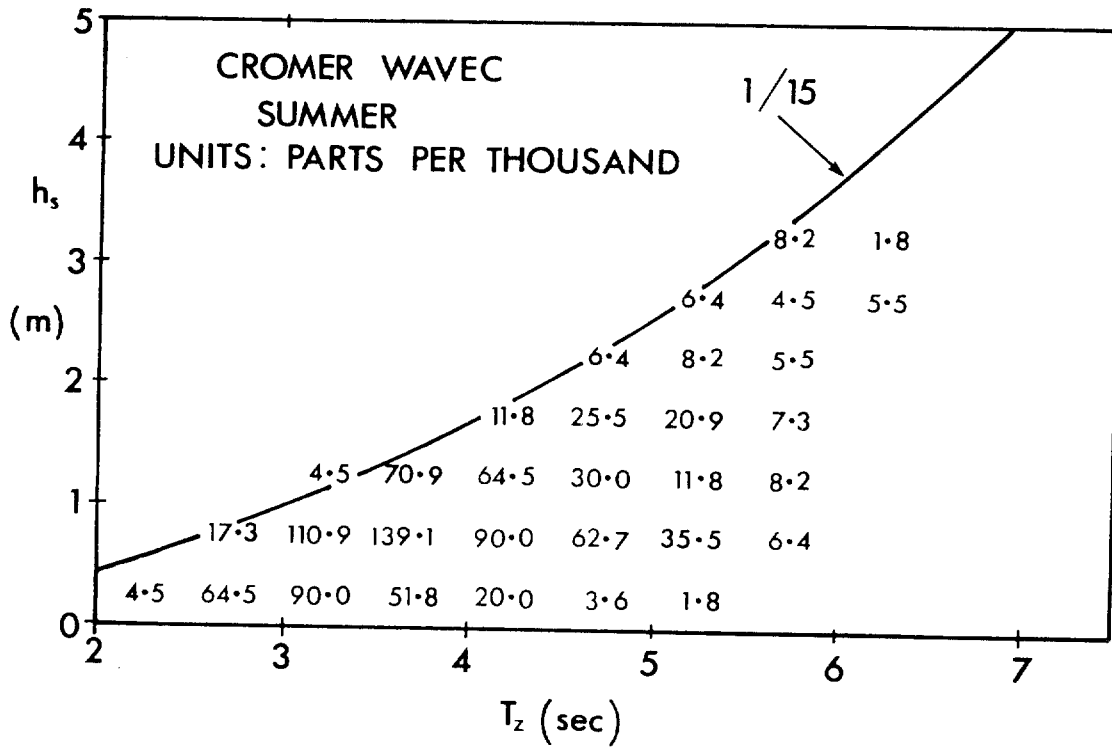


Fig. 5(d)

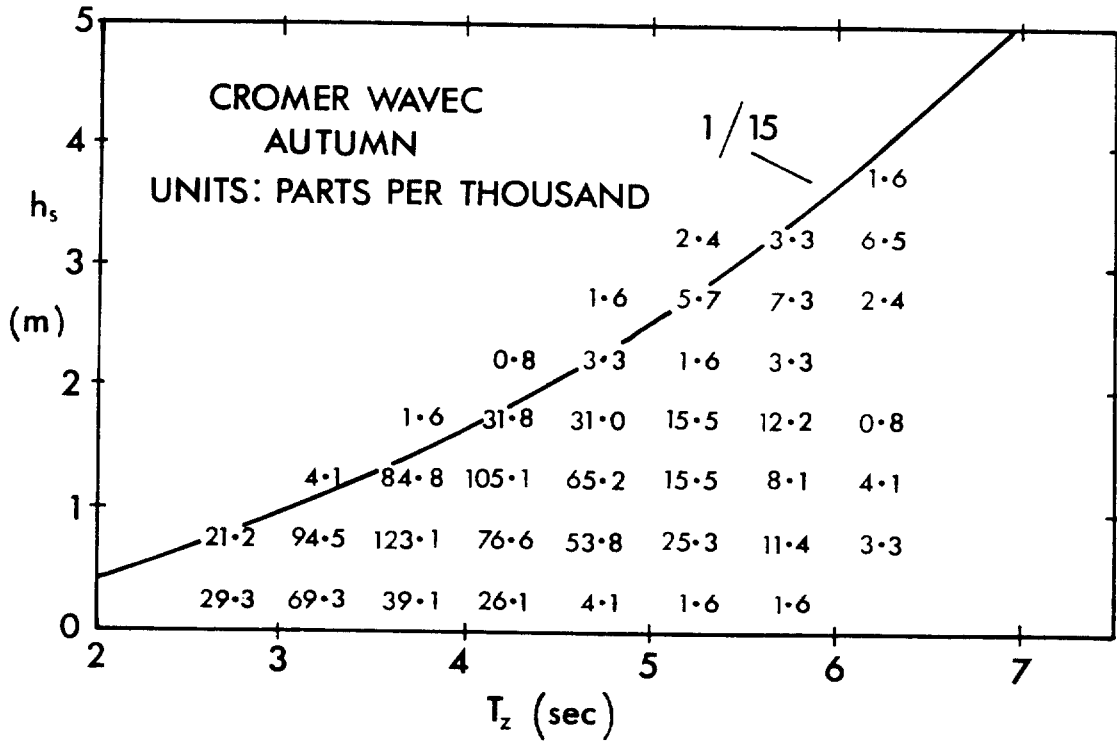


Fig. 5(e)

Fig. 6(a)

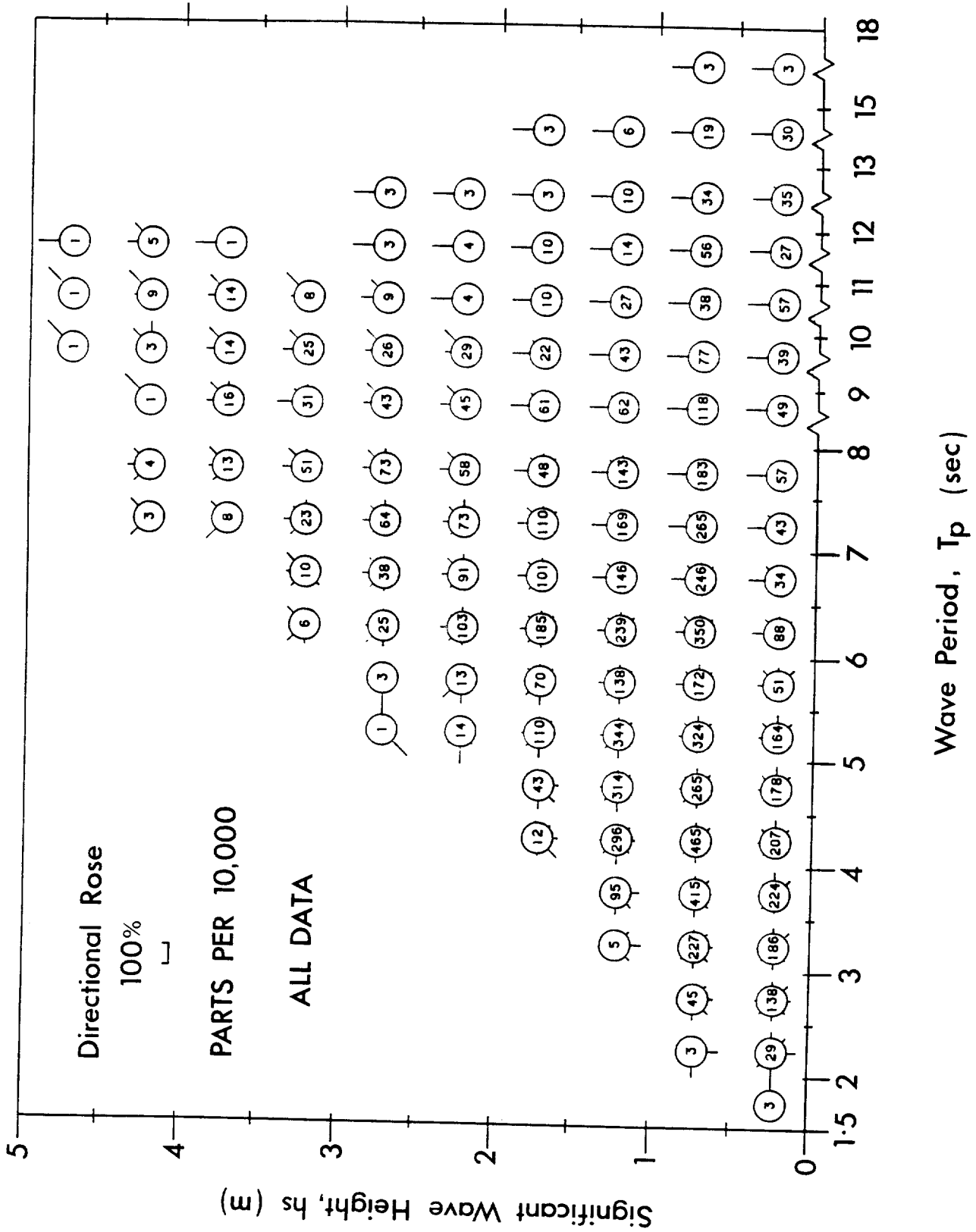




Fig. 6(c)

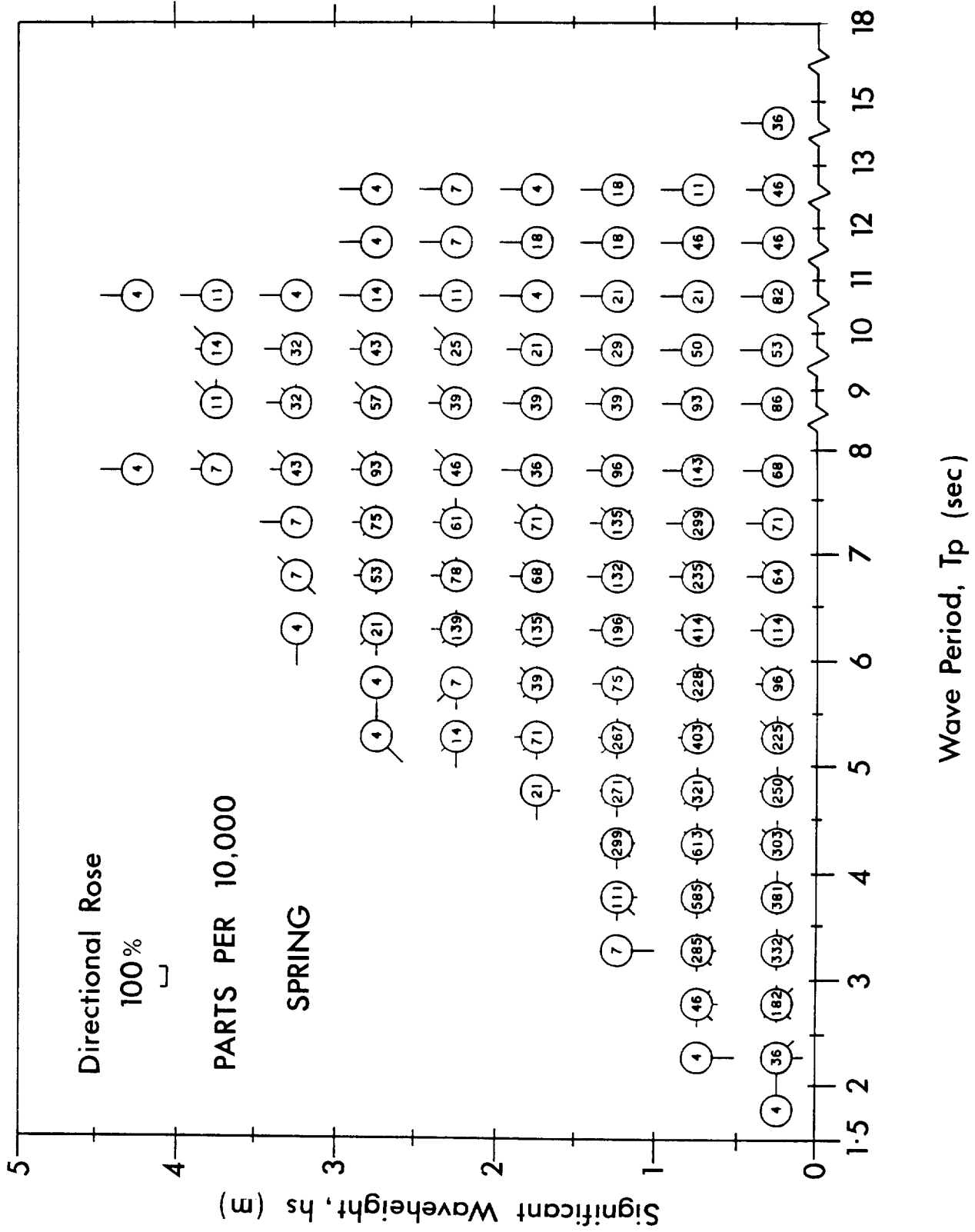


Fig. 6(d)

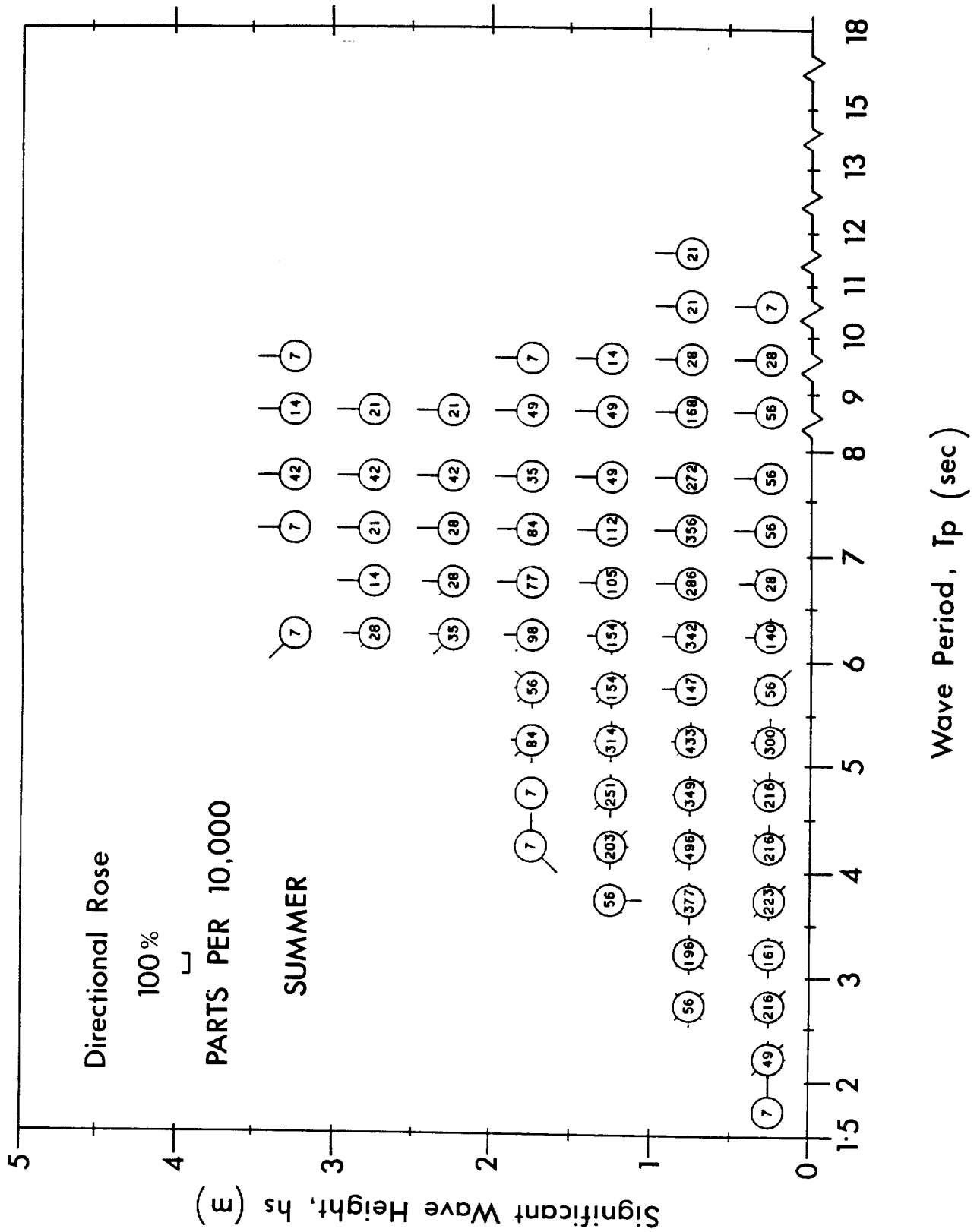
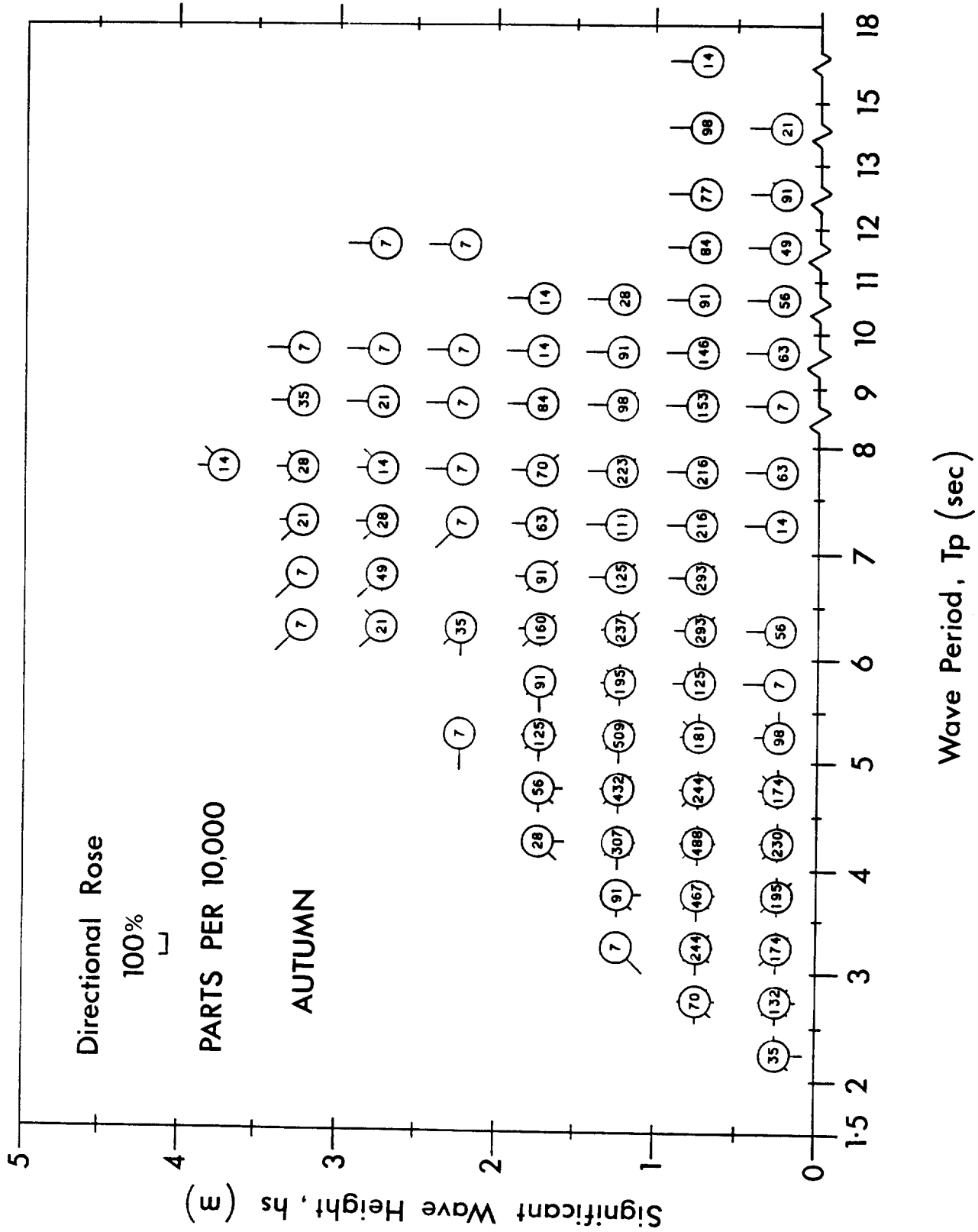


Fig. 6(e)



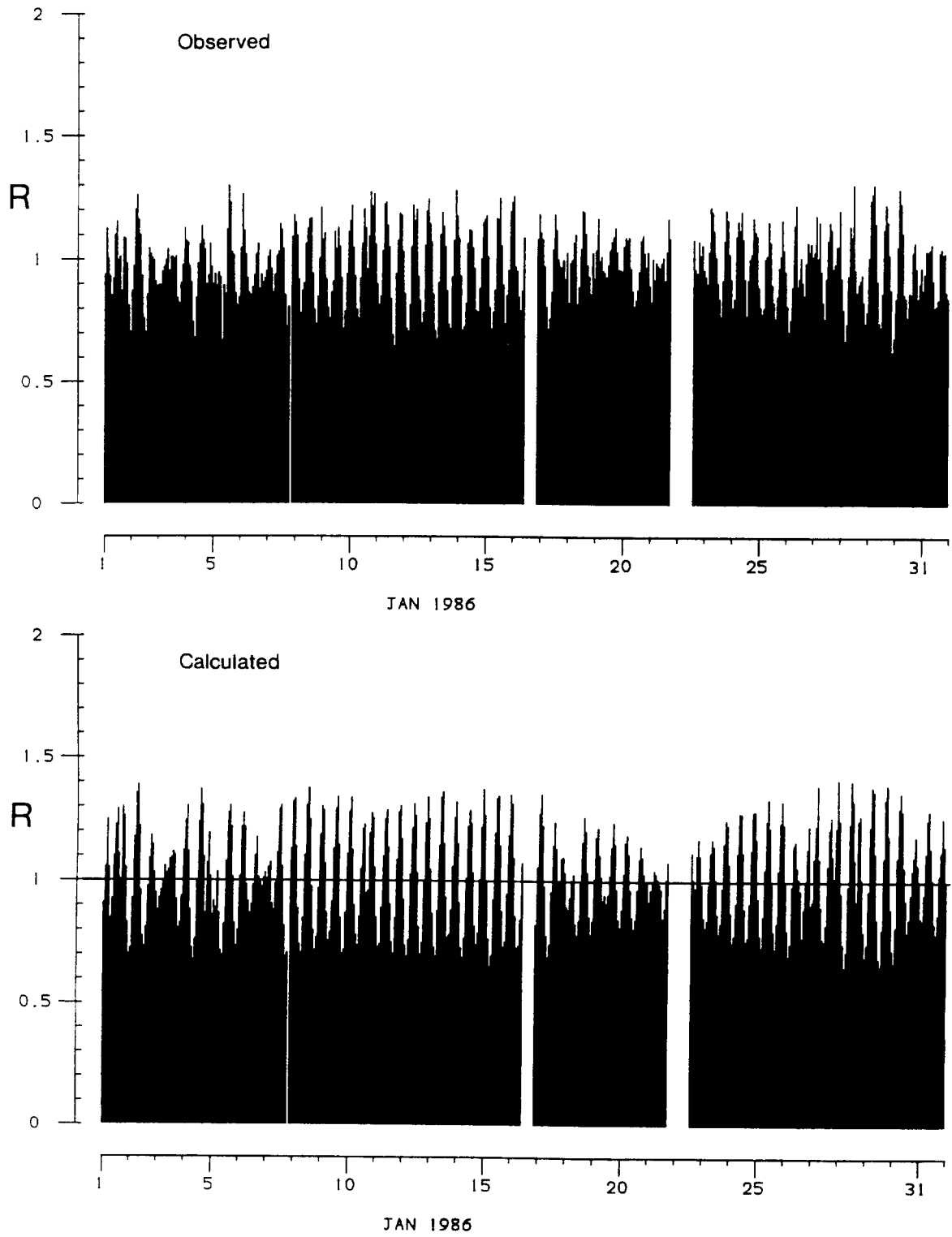


Fig. 7: Comparison of observed values of the check ratio,  $R$ , with values of  $R$  calculated from estimates of the surface current (see Appendix A4).